

Classification and Segmentation of COVID-19 from CT and X-ray Images using Deep Learning Architectures



Author

Hafiz Muhammad Sarmad Khan

NUST CEME 00000274869

Supervisor

Dr. Arslan Shaukat

Department of Computer and Software Engineering

College of Electrical and Mechanical Engineering

National University of Sciences and Technology (NUST)

Islamabad, Pakistan

**Classification and Segmentation of COVID-19 from CT
and X-ray Images using Deep Learning Architectures**

Author

Hafiz Muhammad Sarmad Khan

NUST CEME 00000274869

A thesis submitted in partial fulfillment of the requirements for the
degree of

MS Computer Engineering

Supervisor

Dr. Arslan Shaukat

Thesis Supervisor's Signature: _____

Department of Computer and Software Engineering
College of Electrical and Mechanical Engineering
National University of Sciences and Technology (NUST)
Islamabad, Pakistan

Declaration

I certify that the research titled "*Classification and Segmentation of COVID-19 from CT and X-ray Images Using Deep Learning Architectures*" is my own work. The work was not submitted for assessment elsewhere. The material utilized from external sources has been acknowledged / referred correctly.

Hafiz Muhammad Sarmad Khan
NUST CEME 00000274869

Language Correctness Certificate

This thesis has been proofread by an English expert and is error-free in terms of typing, syntax, semantics, grammatical structure and spelling. The format of the thesis is also prescribed by the university.

Hafiz Muhammad Sarmad Khan

NUST CEME 00000274869

Copyright Statement

- Copyright in text of this thesis rests with the student author. Copies (by any process) either in full, or of extracts, may be made only in accordance with instructions given by the author and lodged in the Library of NUST College of E&ME. Details may be obtained by the Librarian. This page must form part of any such copies made. Further copies (by any process) may not be made without the permission (in writing) of the author.
- The ownership of any intellectual property rights which may be described in this thesis is vested in NUST College of E&ME, subject to any prior agreement to the contrary, and may not be made available for use by third parties without the written permission of the College of E&ME, which will prescribe the terms and conditions of any such agreement.
- Further information on the conditions under which disclosures and exploitation may take place is available from the Library of NUST College of E&ME, Rawalpindi.

Acknowledgment

I am immensely grateful to Allah Almighty for providing me with the patience, direction, and capacity to complete this work. Without HIS blessings I could not have completed my thesis. Indeed Allah is the most merciful and worthy of praise.

I would like to express my gratitude to my supervisor Dr.Arslan Shaukat for their guidance, valuable suggestions and moral support in the entire duration. It's a blessing to have such great people as mentor for research

I am also thankful to the entire thesis committee: Dr. Muhammad Usman Akram and Dr. Sajid Gul Khawaja for their tremendous support and cooperation

My acknowledgment would be incomplete without mentioning my beloved parents without whom I am nothing and who have supported me in every second of my life. I would also like to thank my friends who have always supported me and especially during the research work

Finally, I'd want to convey my thanks to each and every one of my friends and all the individuals who have encouraged and supported me throughout the entire duration.

This thesis is dedicated to my wonderful parents and cherished friends, whose unwavering support and collaboration helped me achieve this magnificent goal.

Abstract

Covid-19 is becoming a significant challenge, with numerous human beings losing their lives every day. Not only a certain country is involved with this outbreak, but even the world has suffered as a result of the coronavirus. Computed Tomography (CT) and X-ray images are resources to the best for COVID-19 screening. It is essential to quickly and accurately classify and segment COVID-19 from CT and X-rays to aid in diagnostic and patient monitoring. Technology today revolutionized the world by using artificial intelligence to replace manual machines with automated ones which enable the system to imitate the human brain by making wise decisions based on experience. This research proposes a comprehensive comparison of deep learning models for CAD (Computer-Aided Design) systems which differentiates between COVID-19 and normal healthy lungs of CT & X-ray images using image classification and segment the radiological images of COVID-19 by using image segmentation. The experimental findings, which were evaluated on a COVID-19 CT and X-ray classification and segmentation dataset, show that deep learning architectures can produce accurate and fast classification and segmentation results on COVID-19, with a maximum accuracy of 98% and 95% for binary and multi-class classification, respectively, and a maximum F1-Score of 98% and 77% for binary and multi-class segmentation, respectively. Deep learning architectures have a strong potential for application in COVID-19 diagnosis.

Keywords: *COVID-19, Deep learning, Image Classification, Image Segmentation, CT, X-rays.*

Contents

1	Introduction	1
1.1	Motivation:	2
1.2	Problem Statement:	2
1.3	Aims and Objectives:	3
1.4	Structure of Thesis:	3
2	Literature Review	5
2.1	Deep learning classification research on COVID-19	6
2.2	Deep learning segmentation research on COVID-19	12
2.3	Research Gap	15
3	Novel Coronavirus (COVID-19)	17
3.1	The Role and Anatomy of Breathtaking Lungs	17
3.1.1	Lungs Anatomy:	17
3.1.2	The Respiratory System:	18
3.1.3	Structure of Lungs:	19
3.1.4	The pathway of breath:	19
3.1.5	How lungs can stay healthy:	19
3.1.6	Lungs disorder and illness:	20
3.1.7	Causes of lung disorders and illnesses:	20
3.1.8	Symptoms to see a doctor:	20

CONTENTS

3.1.9	Lungs function test:	21
3.1.10	Lungs treatment:	21
3.1.11	Tips for healthy lungs:	21
3.2	Medical Imaging	22
3.2.1	CT Scanners:	22
3.2.2	MRI Scanners:	22
3.2.3	Ultrasound:	23
3.2.4	X-ray:	23
3.3	Novel Coronavirus (COVID-19)	23
3.3.1	Causes of COVID-19:	23
3.3.2	Risk factor:	24
3.3.3	Symptoms of COVID-19:	25
3.3.4	COVID-19 Diagnosis:	26
3.3.5	Visual identification of COVID-19 in medical imaging:	26
3.3.6	Prevention:	27
3.3.7	Treatment:	28
3.3.8	When to consult a doctor:	29
3.4	Summary:	29
4	Deep Learning	30
4.1	Background of Deep Learning	30
4.1.1	When to apply DL:	32
4.1.2	Why Deep Learning:	32
4.1.3	Classification of Deep Learning approaches:	32
4.1.4	Types of Deep Learning networks:	32
4.2	Convolutional Neural Network	32
4.2.1	The advantages of using CNN:	33

CONTENTS

4.2.2	CNN Layers:	33
4.3	CNN Architectures	36
4.3.1	CNN Architectures for Classification:	37
4.3.2	CNN Architectures for Segmentation:	41
4.4	Applications of Deep Learning	43
4.5	Evaluation Metrics	44
4.6	Summary	45
5	Methodology	46
5.1	Databases	46
5.1.1	Classification Datasets:	46
5.1.2	Segmentation Datasets:	49
5.2	Proposed Architecture for Classification	50
5.2.1	Proposed Architecture:	51
5.2.2	Transfer Learning:	52
5.2.3	Data Augmentation:	52
5.2.4	Model Hyperparameters:	53
5.2.5	Evaluation Metrics:	53
5.3	Proposed Architecture for Segmentation	54
5.3.1	Proposed Architecture:	55
5.3.2	Data Augmentation:	57
5.3.3	Hyperparameters:	57
5.3.4	Evaluation Metrics:	58
6	Experimental Results	59
6.1	Results	59
6.1.1	Performance of the Binary Class Classification:	59
6.1.2	Performance of the Multi-Class Classification:	63

CONTENTS

6.1.3	Performance of the Binary Class Segmentation:	67
6.1.4	Performance of the Multi Class Segmentation:	67
7	Conclusion	75
7.1	Future Work	76
	References	77

List of Figures

3.1	Structure of lungs [1]	19
3.2	Different medical imaging for lung visualization (a) X-ray (b) CT Scan (c) MRI (d) Ultrasound	24
3.3	Different visual identifications for COVID-19 in medical imaging (a) X-ray (b) CT Scan (c) Ultrasound [2]	27
4.1	Deep Learning Family [3]	31
4.2	Machine Learning vs Deep Learning [4]	31
4.3	CNN Architecture for Image Classification [5]	33
4.4	Convolutional Layer [6]	34
4.5	Pooling Layer [7]	34
4.6	Fully Connected Layer [8]	35
4.7	An example of layered architecture of a basic convolutional neural network [9]	36
4.8	VGG architecture [10]	37
4.9	The Densenet Architecture [11]	38
4.10	Block Diagram of Resnet [12]	38
4.11	Architecture of Mobile net V1 & V2 [13]	39
4.12	The Xception Architecture [14]	39
4.13	The Inception Resnet Architecture [15]	40
4.14	The Efficientnet Architecture [16]	40

LIST OF FIGURES

4.15 Schematic diagram of the NASNet Architecture [17]	41
4.16 The Unet Architecture [18]	41
4.17 The FPN Architecture [18]	42
4.18 The PSPNet Architecture [18]	42
4.19 The LinkNet Architecture [18]	43
4.20 Example of DL Applications [19]	44
5.1 CT Scans of SARS COV II Dataset [20]	47
5.2 CT Scans of COVID CT Dataset [21]	47
5.3 X-ray Scans of COVID Radiography Dataset [22, 23]	48
5.4 X-ray Scans of COVID IEEE-8023 Dataset [24]	48
5.5 Visual Appearance of Medical Segmentation Dataset with Masks [25] . .	49
5.6 Visual Appearance of Zenodo Dataset with Masks [26]	50
5.7 Workflow of COVID-19 Classification	51
5.8 Block Diagram for Training	51
5.9 Block Diagram for Testing	52
5.10 Schema of confusion matrix [27]	54
5.11 Workflow of COVID-19 Segmentation	55
5.12 Block Diagram for Training	56
5.13 Block Diagram for Testing	56
6.1 Confusion Matrix of SARS COV II CT Dataset	60
6.2 Confusion Matrix of COVID-CT Dataset	61
6.3 Confusion Matrix of IEEE 8023 Dataset	62
6.4 Confusion Matrix of X-ray Radiography Dataset	65
6.5 Loss & Accuracy of X-ray Radiography Dataset	66
6.6 Precision, Recall & F1-Score of Multi-class Dataset	66
6.7 Jaccard Index & F1-Score of Binary Class Segmentation	68

LIST OF FIGURES

6.8 Visual Appearance of COVID-19 Segmented Images of Zenodo Dataset	70
6.9 Visual Appearance of COVID-19 Segmented Images of Medical Segmentation Dataset	70
6.10 Ground Truth vs Predicted of COVID-19 Segmentation	72
6.11 Jaccard Index & F1-Score of Multi Class Zenodo Dataset	72
6.12 Jaccard Index & F1-Score of Multi Class Medical Segmentation Dataset	73
6.13 ROC Curves	73

List of Tables

2.1	Literature Review on Classification	11
2.2	Literature Review on Segmentation	16
5.1	Overview of the Classification Datasets	49
5.2	Overview of the Segmentation Datasets	50
5.3	Data Augmentation for Classification	53
5.4	Segmentation Masks	56
5.5	Data Augmentation for Segmentation	57
6.1	Train Test Split for Binary Class Classification	60
6.2	Evaluation Metrics for Binary Classification	63
6.3	Train Test Split for Multi-Class Classification	63
6.4	Evaluation Metrics for Multi class Classification	64
6.5	Overview of methods and quantitative results toward COVID-19 classification	64
6.6	Train Test Split for Binary Class Segmentation	67
6.7	Evaluation Metrics for Binary Segmentation	68
6.8	Train Test Split for Multi-Class Segmentation	69
6.9	Evaluation Metrics for Multi class Segmentation	71
6.10	Comparison of proposed model to various state of the art baseline classification and segmentation approaches	74

CHAPTER 1

Introduction

Many formerly human-dependent processes have been automated by technology, which has revolutionized the environment. Equipment's & technology is present in all spheres of life, from the simplest gadget such as a calculator to massive factory machines. Machines are programmed to execute a series of instructions/commands in order to complete tasks without the need for human intervention. Artificial Intelligence (AI) has revolutionized the world beyond our imagination as technology advances. Machines are trained to imitate the human brain by learning from experience utilizing AI. Usefulness of artificial intelligence (AI) in the medical field has piqued interest, and the first attempt to create a Computer Aided Design (CAD) was made in the 1960s. Artificial intelligence (AI) methods have been utilized in medicine to automate the diagnosis of a variety of diseases. Automatic disease identification has been a hot subject, with many experts contributing to the field by proposing a variety of CAD systems. Such systems assist radiologists in detecting diseases in less time and often serve as a second opinion for radiologists in making the best pathology decisions. However, in order for such systems to make unsupervised decisions, transfer learning is required, which necessitates a vast amount of data, and most medical image datasets have been found to be imbalanced. As a consequence, this research suggests a systematic comparison of deep learning models for CAD systems that employ image classification to distinguish between COVID-19 and normal healthy human lungs in CT and x-ray images, as well as image segmentation to estimate COVID-19's location in CT images.

1.1 Motivation:

Ever since the emergence of COVID-19 which was first discovered in Dec 2019 in Wuhan (China), a lot of individuals & human beings have died from the COVID-19 breakout. Although as most of the victims of the COVID-19 patients and mortalities were reported in China, the World Health Organization proclaimed this outbreak as a Public Health Emergency of International Concern on 30 January 2020, and a pandemic on 11 March 2020 [28]. The cure & medication can take a couple of months due to its clinical experimentation & trials on human being of various age group before acceptance and the treatment may further be postponed due to the virus's potential genetic mutations [29]. New born babies, children, and elderly patients are affecting by SARS-CoV-2. To save more lives, an early diagnosis of any kind of disease, whether contagious and non-contagious is extremely a supreme task. An early screening and fast diagnosing procedure can avoid the spread of epidemic diseases, speed up the related diagnosis and cost-efficient. However, in order for such systems to make unsupervised decisions, transfer learning is required, which necessitates a vast amount of data, and as this disease is relatively new to the world, there most medical image datasets have been found to be imbalanced. As a result, this research suggests systematized comparison of deep learning models for CAD systems that use image classification to distinguish between COVID-19 and normal healthy individuals in CT and x-ray images, as well as image segmentation to determine the position of coronavirus in CT images.

1.2 Problem Statement:

Early diagnosis of any disease, contagious or anti, is vital for effective care and the saving of more lives. An early screening and fast diagnosing process will help prevent the spread of pandemic diseases while also reducing expenses and speeding up the diagnosis process. Many CAD schemes have been suggested for other diseases to date. Since COVID-19 is a novel disorder, the hardest challenge for the researchers is the data availability. Furthermore, the majority of the coronavirus CT and X-ray datasets are inconsistent and unbalanced. As a result, the purpose of this study is to look into and apply various deep learning strategies in order to develop an effective diagnostic method. Not only the deep learning algorithm will speed up the identification process, but it will also relieve

the pressure on doctors and health-care systems.

1.3 Aims and Objectives:

This research can be categorised by following main goals:

- Inspect and equate previous studies on the automated diagnosis of novel coronavirus (COVID-19) and the detection.
- Gathering datasets for COVID-19.
- Proposing a framework for differentiating between normal and COVID-19 images of X-rays and CT scans using deep learning techniques.
- Proposing a segmentation model for identifying the location of COVID-19 images in the CT scans using deep learning techniques.

1.4 Structure of Thesis:

The following is the format of this report:

- **Chapter 2** is a study of previous literature on COVID-19 identification by researchers.
- The lungs, which are an essential organs for respiration, are briefly described in **Chapter 3** along with their anatomy. COVID-19 and its early prevention are also explored in depth.
- **Chapter 4** will cover in-depth awareness of deep learning and its architectures.
- The proposed architecture is detailed in **Chapter 5**. It consists of two major modules: COVID-19 classification in CT scans and X-rays, and COVID-19 semantic segmentation in CT scans.
- The datasets and performance measures used to evaluate the proposed architecture are discussed in **Chapter 6**. Many of the conclusions, as well as the required tables and figures are discussed elaborately.

CHAPTER 1: INTRODUCTION

- This study is wrapped up in **Chapter 7**, which also outlines the thesis's potential / future goals.

CHAPTER 2

Literature Review

More than 100 million cases have been registered worldwide since the outbreak of coronavirus disease 2019 (COVID-19) (formerly known as the 2019 novel coronavirus) in Wuhan, China in December 2019, which is caused by extreme acute respiratory syndrome coronavirus 2 (SARS-CoV-2). This has resulted in a large number of deaths. Despite the fact that the majority of COVID-19 cases and deaths were registered in China, the WHO has designated this epidemic as the world's sixth public health emergency. There is also the possibility of nosocomial infection in hospitalized patients and healthcare staff, as well as virus spread by asymptomatic carriers [30, 31].

Due to the COVID-19, a huge epidemic has now occurred globally, affecting the health and lives of many people all around the world. According to the worldmeter.com, in mid-July 2020, the outbreak had infected over 12 million individuals, resulting in over 570,000 deaths.

Early diagnosis of any illness, contagious or non-infectious, is vital for effective care and the saving of more lives. A quick diagnosis and screening process will help deter the spread of pandemic diseases like SARS-CoV-2, while also cost effective and speeding up the diagnosis process. As computer technology advances, a computer aided device (CAD) can assist in the better diagnosis of illness from chest X-rays and CT scans, as well as provide the radiologist with a second opinion about their diagnosis.

The aim of this literature review is to address a comprehensive survey on the applications of machine learning and deep learning in combating the challenges that COVID-19 has caused. As a result, this literature review will cover some of the concepts and approaches that machine learning and deep learning have addressed so far. Classification

and segmentation are the techniques and approaches used, and they have been validated on publicly accessible datasets. Images from CT scans and X-rays are used in the dataset.

2.1 Deep learning classification research on COVID-19

To construct a medical image classification model, features are extracted from the dataset and a classifier is trained on those features to distinguish between normal and abnormal instances, much like any other classification issue. COVID-19 grouping has been the subject of many studies. The following is a summary of the published work in this area.

In [32], *Tuan D. Pham* proposed a research on 16 pre-trained COVID-19 COnvolutional Neural Networks based on the wide-ranging public collection of CT scans from the COVID-19 and non-COVID-19 patients is described in this study. The database consists of 349 CT images containing clinical findings of COVID-19 from 216 patients, and 397 CT images obtained from non-COVID-19 subjects. These CT images were collected from COVID19-related papers published in medRxiv, bioRxiv, NEJM, JAMA, Lancet, and others. The dataset was randomly Split into 80% for training and 20% for testing. The results were presented with mean accuracy of 93% with data augmentation and 96% without data augmentation.

In [33], *T.Ozturk, M.Talo* et al proposed a model providing diagnostics for binary classification (COVID vs. No-Findings) and multi-class classification (COVID vs. No-Findings vs. Pneumonia). The Dark Net model was used in their study as a classifier for “you only look once (YOLO)” real time object detection system. In this study, X-ray images obtained from two different sources were used for the diagnosis of COVID-19. Their model produced a classification accuracy of 98.08% for binary classes and 87.0% for multi-class cases.

In [34], *Asif Iqbal Khan* et al proposes CoroNet, a Deep Convolutional Neural Network model to automatically detect COVID-19 infection from chest X-ray images. The proposed model is based on Xception architecture pre-trained on ImageNet dataset and trained end-to-end on a dataset prepared by collecting COVID-19 and other chest pneumonia X-ray images from two different publicly available databases. CoroNet has been

trained and tested on the prepared dataset and the experimental results show that their proposed model achieved an overall accuracy of 89.6% for 4-class cases (COVID vs Pneumonia bacterial vs pneumonia viral vs normal). For 3-class classification (COVID vs Pneumonia vs normal), the proposed model produced a classification accuracy of 95% and 99% for binary classification (COVID vs normal).

Tanvir Mahmud et al in [35] proposed a deep convolutional neural network (CNN) based architecture, named as CovXNet, is proposed that utilizes depth wise convolution with varying dilation rates for efficiently extracting diversified features from chest X-rays. One of the datasets used in this study is a collection of total 5856 images consisting 1583 normal X-rays, 1493 non-COVID viral pneumonia X-rays and 2780 bacterial pneumonia X-rays collected in Guangzhou Medical Center, China. Another database containing 305 X-rays of different COVID-19 patients is collected from Sylhet Medical College, Bangladesh which is also verified by expert radiologist panel. Finally, a smaller balanced database is created combining all the COVID-19 X-rays with equal number of normal, viral, bacterial pneumonia X-rays (305 X-rays in each class) that are employed for the transfer learning phase. The rest of the X-rays (Normal, viral, bacterial pneumonia) are utilized for the initial training phase. In both these phases, five-fold cross validation scheme is employed for the evaluation of the proposed method. CovXNet detect COVID-19 and other types of pneumonia with distinctive localization from chest X-rays. Instead of using traditional convolution, efficient depth wise convolution is used with varying dilation rates that integrates features from diversified receptive fields to analyze the abnormalities in X-rays from different perspectives. Extensive experimentation using two different datasets provide very satisfactory detection performance with accuracy of 97.4% for COVID/Normal, 87.3% for COVID/Viral pneumonia, 94.7% for COVID/Bacterial pneumonia, 89.6% for multi class COVID/Viral/Bacterial pneumonia and 90.2% for multi class COVID/normal/Viral/Bacterial.

In [36], *Alejandro R. Martinez* proposed Multi-Source Transfer Learning (MSTL) to build on traditional Transfer Learning for the classification of COVID-19 from CT scans, using four pretrained models from Tensorflow's Kera's API: ResNet50V2, ResNet101V2, DenseNet121, and DenseNet122. The models outperformed baseline ImageNet fine-tuned models thanks to their multi-source fine-tuning strategy. Moreover, he also suggested an unsupervised label creation method for their Deep Residual Networks, which improves their efficiency. The model was able to reach a 89% accuracy rate.

Hammam Alshazly et al in [37] proposed some deep learning-based methods for detecting COVID-19 using chest CT images. The most sophisticated deep network architectures and their variants were considered, and detailed tests were carried out on the two datasets with the most CT images available to date "SARS COV 2 and COVID-19 CT". Furthermore, they looked at various configurations and determined a custom-sized input for each network to get the excellent outcomes. The COVID-19 detection performance of the resulting networks was greatly improved. On the SARS CoV-2 CT and COVID19-CT datasets, their models achieved state-of-the-art performance with average accuracy's of 99.4% and 92.9% respectively.

In [38], *Bin Liu et al* developed a lesion-attention deep neural network (LA-DNN) to predict COVID-19 positive or negative with a richly annotated chest CT image dataset. They extract two forms of valuable information for the annotations from the textual radiological report that comes with each CT image: One is an indicator for whether a COVID-19 case is positive or negative, and the other is a description of five lesions on CT images consistent with positive cases. The suggested data-efficient LADNN model focuses on the primary role of binary classification for COVID-19 diagnosis, while concurrently implementing an auxiliary multi-label learning task to attract the model's attention to the five lesions identified with COVID-19. The area under the curve (AUC), sensitivity (recall), specificity, and accuracy for COVID-19 diagnosis was 94.0%, 88.8% , 87.9% , and 88.6% respectively according to the experimental results which meet clinical criteria for realistic application.

In [39], *D. M. H. Nguyen et al* proposed a novel method for improving COVID-19 diagnosis using deep learning-based systems. Unlike previous research, they were motivated by radiologists' decisions while evaluating COVID-19 patients and as a result, pertinent data such as contaminated regions or heat-maps of the injury area were evaluated for the final decision. Extensive testing revealed that using all visual cues improves the efficiency of many baselines, including two of the best network architectures (ResNet50 and DenseNet169) and three other states of the arts from recent works achieving an accuracy of 89%.

In [40], *Md. Kamrul Hasan et al* proposed the CVR-Net (Coronavirus Recognition Network) in this article as a robust CNN-based network for the automated recognition of the coronavirus from CT or X-ray images. The proposed end-to-end CVR-Net is a

multi-scale-multi-encoder ensemble model, in which the outputs of two different encoders and their different scales have been combined to achieve the final prediction probability. The model was learned and validated on three separate datasets, all of which included images gathered from various open-source repositories. They compare the proposed CVR-Net to current approaches that were trained and tested on the same dataset as the proposed CVR-Net. Their model achieved an average F1-score and accuracy of 0.997 0.998; 0.963 0.964; 0.816 0.820; 0.961 0.961; and 0.780 0.780.

In [41], *Xiang Yu et al* proposed CGNet, a deep learning system for a binary classification challenge that distinguishes between regular and pneumonia chest X-ray images. On a public pneumonia dataset of 5,856 chest X-ray images, their model had the best accuracy of 0.9872, sensitivity of 1, and specificity of 0.9795. They also put the suggested approach to the test on a publicly available COVID-19 CT dataset, with the best results of 0.99% accuracy, 1% specificity, and 0.98% sensitivity, respectively.

Muhammad E. H. Chowdhury in [22] proposed a robust method for detecting COVID-19 pneumonia from automated chest X-ray images using pre-trained deep-learning algorithms with the highest detection accuracy. The authors built an online database by merging many public databases and extracting images from recently published journals. There are 423 COVID-19, 1485 viral pneumonia, and 1579 normal chest X-ray images in the database. Several pre-trained deep Convolutional Neural Networks were trained and validated using the transfer learning methodology and image augmentation (CNNs). The networks was trained to distinguish between two types of pneumonia: i) Normal and COVID-19 pneumonia; and ii) normal, bacterial and COVID-19 pneumonia with and without image augmentation. Both systems had 99.7% and 97.9% classification accuracy respectively.

Michael J. Horry et al in [42] demonstrated that the VGG19 model could be used to build appropriate deep learning-based tools for COVID-19 detection using existing small and challenging COVID-19 datasets. For various imaging modes, including X-Ray, Ultrasound, and CT scan, the model will classify both Pneumonia vs Normal and COVID-19 vs Pneumonia conditions. With accuracy of up to 86% for X-Ray, 100% for Ultrasound, and 84% for CT scans, the chosen VGG19 model performs in significant levels of COVID-19 detection against pneumonia or standard for all three lung image modes.

Siti Raihanah Abdani et al in [43] proposed a simple deep learning model called SPP-COVID-Net for correctly screening the probability of COVID-19. The proposed model uses a modified spatial pyramid pooling module and 14 layers of convolutional neural networks. The suggested SPP-COVID-Net achieves the highest mean accuracy of 94% with the lowest standard deviation among the training folds accuracy, according to the output data. It has only 862,331 cumulative parameters and needs fewer than 4 Mb of memory bandwidth. The model is well-suited to be used for rapid screening in order to perform better-targeted diagnoses and reduce test time and expense.

Using a chest X-ray image, the research in [44] employs a versatile and effective deep learning technique, utilizing the CNN model in predicting and detecting a patient unaffected and affected with the disease. To demonstrate the accuracy of the CNN model being trained, the researchers used a dataset of 20,000 images with a 224x224 image resolution and 32 batch scale. During the success training, the trained-model achieved a 95% accuracy score. The research work will diagnose and forecast COVID-19, bacterial, and viral-pneumonia diseases based on chest X-ray images based on the results of testing.

In [45], *Prabira Kumar Sethy* et al developed a deep feature and SVM-based technique for detecting coronavirus (COVOD-19) using X-ray images. They did this by extracting the deep features of 13 pre-trained CNN models and feeding them to the SVM classifier one by one. Each classification model is tested 20 times and the average value is reported to improve the robustness of the classification model. In comparison to the other 12 classification models, the ResNet50 + SVM classification model performs well. The proposed classification model for COVID-19 identification has a 95.33% accuracy rate. The accuracy of 95.33% is based on the average of 20 independent executions, with a maximum value of 98.6%.

In [46], COVID-Net, an open source and publicly accessible deep convolutional neural network architecture tailored for the identification of COVID-19 cases from chest X-ray (CXR) images was introduced in this study. They also introduced COVIDx, an open-access benchmark dataset made up of 13,975 CXR images from 13,870 patient cases, with the highest number of publicly accessible COVID-19 positive cases to the authors' awareness. The mode; was able to achieve a highest accuracy of 94% with VGG-19 and Resnet-50 in comparison.

CHAPTER 2: LITERATURE REVIEW

Table 2.1: Literature Review on Classification

Author	Year	Dataset	Techniques	Results "Accuracy"
Tuan D. Pham	2020	COVID CT Dataset	16 pre-trained Convolutional Neural Network	93% with data augmentation 96% without data augmentation
Tulin Ozturk	2020	Local COVID-19 X-ray Dataset	Darknet Classifier	98 % binary class 87% multi-class
Asif Iqbal Khan	2020	Local COVID-19 X-ray dataset	Coronet Classifier	90% 4-class 95% 3-class 99% binary class
Tanvir Mahmud	2020	Local COVID-19 X-ray dataset	Covxnet CLassifier	97% COVID vs Normal 87% COVID vs Viral Pneumonia 94% COVID vs Bacterial Pneumonia 89% COVID vs Bacterial vs Viral 90% COVID vs Normal vs Bacterial vs Viral
Alejandro R. Martinez	2020	Local COVID-19 CT Dataset	Multi Source Transfer Learning (MSTL)	89%
Hammam Al-shazly	2021	SARS COV 2 CT Dataset COVID CT Dataset	Deep learning based methods	99% 92%
Bin Liu	2020	Local COVID-19 CT Dataset	Lesion-attention deep neural network (LA-DNN)	89%
D. M. H. Nguyen	2020	Local COVID-19 CT Dataset	Deep Learning Models	89%
Md. Kamrul Hasan	2020	3 Local Datasets	CVR-Net (Coronavirus Recognition Network)	91%
Xiang Yu	2021	Local COVID-19 X-ray Dataset	CGNet	99%
Muhammad E. H. Chowdhury	2020	Local COVID-19 Xray Dataset	Pre-trained deep Convolutional Neural Networks	99% with data augmentation 97% without data augmentation
Michael J. Horry	2020	Local COVID-19 CT, X-ray and Ultrasound Dataset	VGG-19	86% X-ray 100% Ultrasound 84 % CT
Siti Raihanah Abdani	2020	Local COVID-19 Dataset	SPP-COVID-Net	94%
Sammy V	2020	Local COVID-19 X-ray Dataset	CNN Model	95%
S.Prabira Kumar Sethy	2020	Local COVID-19 X-ray Dataset	Deep Features and SVM	95%
Linda Wang	2020	Local COVID-19 X-ray Dataset	COVID-Net	94%

2.2 Deep learning segmentation research on COVID-19

In the healthcare sector, image segmentation is still widely used for medical imaging research. It is used in the diagnosis of multiple illnesses for deep learning to figure out the exact illness by computer vision and forecast future consequences, allowing physicians to make quicker care decisions. Several experiments were performed in order to develop an automatic COVID-19 segmentation process. The biggest obstacle though is obtaining the dataset for segmentation. Researchers in this area have done excellent work which is briefly explained in this section.

In [47], *Narges Saeedizadeh* et al suggested a segmentation framework for detecting COVID-19-infected chest regions in CT images. They used a TV-Unet architecture which is similar to the U-Net model, to train it to detect ground glass regions at the pixel level. Their experimental study which included everything from visual evaluation of predicted segmentation outcomes to quantitative assessment of segmentation performance (precision, recall, Dice score, and mIoU) revealed that they were able to accurately identify COVID19-associated lung areas with a mIoU rating of over 99% and a Dice score of about 86%.

Adnan Saood in [48] proposed two deep learning networks "U-Net & SegNet" for COVID-19 lung CT image segmentation. Both networks were used as multi-class segmentors as well as binary segmentors. Seventy-two data images were used to train each network, which was then validated on ten images before being tested against the remaining eighteen images. For the results, several statistical ratings were estimated and tabulated. The results show that SegNet outperforms the other methods in classifying infected/non-infected tissues with 95% accuracy, while the U-NET outperforms the others as a multi-class segmentor with 91% accuracy.

Instead of using modern or computationally complex neural network architectures, *Dominik Müller* in [49] used a traditional 3D U-Net architecture. They were able to construct a highly accurate and stable segmentation model for lungs and COVID-19 infected regions using a 5-fold cross-validation on 20 CT scans of COVID-19 patients without overfitting on the small data by using a 5-fold cross-validation on 20 CT scans of COVID-19 patients. Dice similarity coefficients of 95% for lungs and 76% for infection was achieved using their system. They demonstrated that the developed system outperforms competing methods, advances the state-of-the-art in COVID-19 segmentation,

and enhances medical image analysis with minimal data.

In [50], *A. Amyar* et al proposed a multitask deep learning model to jointly classify COVID-19 patients and segment COVID-19 lesions from chest CT images. A dataset of 1044 patients is used to evaluate and compare the proposed model with other image segmentation and classification methods, including 449 patients with COVID-19, 100 healthy patients, 98 patients with lung cancer, and 397 patients with various pathologies. The obtained results reveal that their system performs admirably, with a dice coefficient of 0.78% for segmentation and a classification area under the ROC curve of more than 93%.

In [51], *Athanasios Voulodimos* et al examined the efficacy of deep learning models for semantic segmentation of pneumonia contaminated region segmentation in CT images for COVID-19 detection in this research. They used real-world CT data from COVID-19 patients to test the effectiveness of U-Nets and Fully Convolutional Neural Networks in this task. The findings show that Fully Convolutional Neural Networks can accurately segment despite the dataset's class imbalance and man-made annotation errors on the boundaries of symptom manifestation regions, and that they may be a promising method for further study of COVID-19-induced pneumonia symptoms in CT images.

In [52], *Kai Gao* et al developed a dual-branch combination network (DCN) for COVID-19 diagnosis that can achieve individual-level classification and lesion segmentation at the same time in this study. A new lesion attention module was developed to integrate the intermediate segmentation results and focus the classification branch more intensely on the lesion areas. They used a broad dataset of 1,202 subjects from ten Chinese institutes in their research. The findings showed that the proposed DCN outperformed other models with a accuracy of 96.74% on the internal dataset and 92.87% on the external validation dataset.

In [53], MiniSeg, a lightweight deep learning model for effective COVID-19 segmentation was proposed. MiniSeg has many important advantages over conventional segmentation methods: i) It only has 83K parameters, making it difficult to overfit; ii) It has a high numerical reliability, making it suitable for realistic deployment; and iii) It can be quickly retrained by other users using their own COVID-19 data to improve performance even more. Furthermore, they establish a COVID-19 segmentation benchmark to compare MiniSeg to conventional approaches. The model received an 85% IOU ranking.

In [54], The Attention Gate-Dense Network- Improved Dilation Convolution-UNET is a recent COVID-19 pulmonary infection segmentation depth network proposed in this paper by *Alex Noel Joseph Raj* et al. To improve feature propagation and solve the gradient disappearing problem, the dense network replaces convolution and the maximum pooling function. To obtain further edge features from the limited infected areas, an enhanced dilation convolution is used to increase the receptive field of the encoder performance. The addition of an attention gate to the model reduces background noise and increases prediction accuracy. The ADID-UNET model will reliably segment COVID-19 lung infected areas, according to the findings of the experiments. The experimental results indicate that the ADID-UNET model can reliably segment COVID-19 lung infected regions with Accuracy, Specificity, and Dice Coefficient efficiency measures exceeding 80%. (DC). Furthermore, as compared to other state-of-the-art architectures, the proposed model demonstrated excellent segmentation results scoring 80% and 82% respectively on the DC and F1 scales.

In [55], *Tongxue Zhou* et al proposed an automatic COVID-19 CT segmentation network using spatial and channel attention mechanism. They suggested that a U-Net architecture implement an attention structure that includes both spatial and channel attention to re-weight the feature representation spatially and channel-wise to capture rich contextual interactions for improved feature representation. The experiment results, which were tested on a COVID-19 CT segmentation dataset with 473 CT slices, show that the proposed method can accurately and quickly segment COVID-19 data. A single CT slice can be segmented in 0.29 seconds using this tool. The Dice Score, Sensitivity, and Specificity received was 83.1, 86.7, and 99.3 percent, respectively.

In [56], *Omar Elharrouss* et al proposed a COVID-19 lung infection segmentation system. Using encoder-decoder networks on CT-scan images, computer vision techniques are used to distinguish the contaminated regions of the lungs in COVID-19 patients. Different types of segmentation have been used including binary and multi-class segmentation of contaminated lung areas. The experiment demonstrates accurate segmentation of the lung infection area in both binary and multi-class segmentation while comparing the proposed approach to the state-of-the-art process. The model has achieved and overall F1-score of 78% for binary segmentation and 64% for multi-class segmentation.

In [57], *Yu-Huan Wu* et al proposed a novel Joint Classification and Segmentation (JCS)

method for performing COVID-19 chest CT diagnosis in real time and with explanations. They built a large-scale COVID-19 Classification and Segmentation (COVID-CS) dataset with 144,167 chest CT images of 400 COVID-19 patients and 350 uninfected cases to train their JCS system. Fine-grained pixel-level labels with opacifications, which are expanded attenuation of the lung parenchyma, are annotated on 3,855 chest CT images of 200 patients. They also have annotated lesion counts, opacification sites, and positions which helps with different aspects of diagnosis. Extensive tests show that the proposed JCS diagnostic scheme is very effective at classifying and segmenting COVID-19. On the classification test experiment, it achieves an average sensitivity of 95% , a specificity of 93.0% and a Dice score of 78.5% on the segmentation test set of their COVID-CS dataset.

2.3 Research Gap

Some of the research gaps in the existing literature are summarized below:

- Data is the first step to developing any diagnostic/prognostic tool. That is why the most difficult challenge for the researchers was obtaining the dataset.
- Many researchers used a proprietary dataset, making it impossible to do additional analysis.
- Although vast public databases of more common chest X-rays and CT scans exist, there is no such database of COVID-19 chest X-rays or CT scans optimized for computational research.
- Since COVID-19 is a global pandemic, the quality of images was degraded when creating a public dataset of X-ray and CT scans, thereby making diagnostic decisions less precise. The Hounsfield unit (HU) values are decreased, the amount of bits per pixel is diminished, and image resolution is reduced as a result of the content loss.

CHAPTER 2: LITERATURE REVIEW

Table 2.2: Literature Review on Segmentation

Author	Year	Dataset	Technique	Results
Narges Saeed-izadeh	2021	Local COVID-19 Dataset	TV-Unet	IOU = 99% Dice Score = 86%
Adnan Saood	2021	Local COVID-19 Dataset	U-Net & SegNet	Acc = 95% "Binary class Segmentation" Acc = 91% "Multi-class Segmentation"
Dominik Müller	2020	COVID-19 CT Lung and Infection Segmentation Dataset	3D-Unet	Dice Score = 95% "Lungs" Dice Score = 76% "COVID-19 Infection"
A. Amyar	2020	Local COVID-19 Dataset	Multitask Deep learning model of classification & segmentation	Dice Score = 78% ROC = 93%
Athanasiou Voulodimos	2020	Local COVID-19 Dataset	U-Net & FCN "Fully Convolutional Neural Network"	F1-Score = 55% "U-net" F1-Score = 65% "FCN"
Kai Gao	2021	Board CT Dataset acquired from 10 Chinese Institutes	Dual Branch Combination Network	Acc = 92%
Yu Qiu	2021	Local COVID-19 Dataset	Miniseg	IOU Score = 85%
YuAlex Noel Joseph Raj	2021	Local COVID-19 Dataset	Attention Gate-Dense Network-Improved Dilation Convolution-UNET "ADID U-Net"	Dice Score = 80% F1-Score = 81%
Tongxue Zhou	2020	Local COVID-19 Dataset	Automatic COVID-19 CT segmentation network using spatial and channel attention mechanism	Dice Score = 83%
Omar Elharrouss	2020	Local COVID-19 Dataset	Encoder Decoder Network	F1-Score = 78% "Binary class Segmentation" F1-Score = 64% "Multi-class Segmentation"
Yu-Huan Wu	2021	Private Dataset	Joint Classification & Segmentation "JCS"	Dice Score = 78%

CHAPTER 3

Novel Coronavirus (COVID-19)

The heart, brain, liver, kidney, and lungs are the five organs in the human body that are absolutely necessary for life. Lungs are the most important organs of the respiratory system, and the mixing of carbon dioxide and oxygen between the body and the environment is the force that keeps it running. The anatomy and imaging techniques for the lungs will be explored in this chapter, as well as a brief introduction to the Novel Coronavirus (COVID-19).

3.1 The Role and Anatomy of Breathtaking Lungs

The respiratory (breathing) mechanism is focused on the lungs. To remain alive and well, every cell of the body requires oxygen. Carbon dioxide must therefore be expelled by the body. This gas is a waste product generated by cells as part of their routine functions. Any time you take a breath in or out, your lungs are programmed to swap these gases. Let's look at this complicated device in greater detail [58].

3.1.1 Lungs Anatomy:

This spongy, pinkish organ in your chest resembles two upside-down cones. Three lobes make up the right lung. To make way for the heart, the left lung has just two lobes.

The bottom of the trachea is where your lungs begin (windpipe). The trachea is a conduit that allows oxygen to enter and exit the lungs. A tube called a bronchus attaches each lung to the trachea. In the chest, the trachea and bronchi airways form an upside-down "Y." The bronchial tree is the name given to this "Y."

CHAPTER 3: NOVEL CORONAVIRUS (COVID-19)

The bronchi divide into smaller bronchi and bronchioles, which are also smaller tubes. These tiny tubes branch out into every part of the lungs like the roots of a tree. They're so little that some of them are the thickness of a feather. Each lung contains nearly 30,000 bronchioles.

The alveoli are a cluster of small air sacs at the end of each bronchiole channel (individually referred to as alveolus). They resemble grape bunches or very little balloons. In your lungs, there are about 600 million alveoli. The lungs have a surprising amount of surface space, similar to a tennis court, thanks to the tiny bubble forms of the alveoli. This indicates that there is sufficient space for vital oxygen to enter your body.

3.1.2 The Respiratory System:

The key component of the respiratory system is the lungs. The upper respiratory tract and the lower respiratory tract make up this system.

The upper respiratory tract consists of the following organs:

- The human mouth and nose are two separate components of the body. Air enters and exits the lungs through the mouth and nostrils of the nose.
- Nasal Cavity: The air enters the nose first, then the nasal cavity, then the lungs.
- Throat (pharynx): Air is carried from the mouth into the lungs through the throat.
- Voice box (larynx): The throat aids in the passage of oxygen through the lungs while keeping the food and drink out.

The lower respiratory tract is made up of the following components:

- | | |
|----------------------|---------------------------|
| • Lungs | • Bronchi and Bronchioles |
| • Trachea (Windpipe) | • Alveoli |

When people breathe, other portions of the respiratory system assist the lungs in expanding and contracting. The ribs around the lungs, as well as the dome-shaped diaphragm muscle behind them, are included.

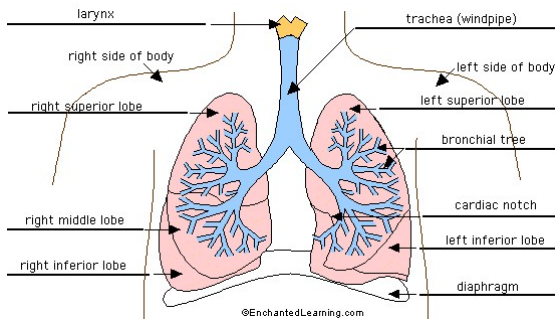


Figure 3.1: Structure of lungs [1]

3.1.3 Structure of Lungs:

3.1.4 The pathway of breath:

Air reaches the mouth and nose when people respire and travel as follows:

- Down the throat and then into the trachea
- The right and left main bronchi in the lungs
- Then into the small bronchi airways
- Into the even smaller bronchi tubes
- Finally, Into the alveoli

A net of tiny blood vessels called capillaries covers each alveolus. Here, oxygen and carbon dioxide are exchanged. The lungs receive deoxygenated blood from your heart. This is carbon dioxide-carrying blood rather than oxygen-carrying blood. The alveoli provide oxygen to the blood as it flows into the narrow, thin-walled capillaries. Carbon dioxide is returned to the alveoli through the thin walls. The heart pumps oxygen-rich blood back to the lungs, and is then pumped around the body. Carbon dioxide is exhaled from the mouth and nose from the lungs and alveoli.

3.1.5 How lungs can stay healthy:

And as human being exhale air, the alveoli remain partially inflated like a balloon. Surfactant is a fluid produced by the lungs to keep them open. Surfactant also includes fatty proteins that aid in the proper functioning of the lungs.

CHAPTER 3: NOVEL CORONAVIRUS (COVID-19)

The lungs disinfect themselves.

Mucus are produced to capture germs and particles. Cilia, thin hairs that cover the airways, and sweep away the mucus. This mucus is normally swallowed without your knowledge. The lungs can produce too much mucus if someone have a respiratory illness.

Macrophages, which are immune cells, are also found in the alveoli. Until germs and irritants will create an infection in your lungs, these cells "kill" them.

3.1.6 Lungs disorder and illness:

A respiratory problem may be acute or chronic (long term). Some forms may lead to lung disease or be a symptom of it. The following are examples of common lung diseases:

- Asthma
- Pneumonia
- Bronchitis
- Tuberculosis (TB)

3.1.7 Causes of lung disorders and illnesses:

Breathing difficulties may be caused by respiratory or lung conditions. In most countries, they are a frequent cause for doctor visits. A human being can get respiratory illness due to:

- Bacteria
- Chemicals
- Virus
- Stagnant indoor air
- Mold
- Tobacco, cigarettes
- Polluted air
- Allergies like pollen, dust, food

3.1.8 Symptoms to see a doctor:

The American Lung Association lists the following early symptoms of lung disease:

- Chronic cough that lasts for a month or longer
- Shortness of breath after little or no exertion
- Wheezing or noisy breathing

CHAPTER 3: NOVEL CORONAVIRUS (COVID-19)

- Chronic mucus or sputum in your lungs that lasts for a month or longer
- Chronic chest pain that lasts for a month or longer
- Coughing up blood

3.1.9 Lungs function test:

If human being have a respiratory disorder, they may need scans to determine how well their lungs are doing. They will also aid in the diagnosis of chronic lung disease. For those with chronic illnesses like asthma, some of these tests are normal. The following are some of the most popular lung function examinations and scans:

- Arterial blood gas test
- Blood test
- Chest x-ray
- Exhaled nitric oxide test
- Lung diffusion test
- Mucus sample

3.1.10 Lungs treatment:

Some treatments for respiratory issues include:

- Antibiotics
- Anti-viral medication
- Anti-fungal medication
- Heart burn drugs
- Synthetic surfactant drugs
- Immune system medication

3.1.11 Tips for healthy lungs:

Although the body has a mechanism in place to keep the lungs safe, there are a few things people can do on a daily basis to either reduce the chance of lung cancer or alleviate symptoms:

- Don't smoke
- Don't chew tobacco
- Get vaccinated against the flu and pneumonia, especially if you have asthma

- Get regular aerobic exercise, such as walking and jogging, to help improve your lung capacity.
- Consider using an air purifier indoors to reduce air pollution from dust, pet dander, and chemicals.
- Wash your hands with soap and water several times a day, etc

3.2 Medical Imaging

Medical imaging refers to the use of imaging modalities and procedures to obtain images of the human body that can aid in patient care and care. It can also be used to keep track of any chronic conditions, and can aid treatment plans. There are several types of medical imaging methods, each of which utilizes a particular technology to generate images for various purposes mentioned below:

3.2.1 CT Scanners:

A computerized tomography scan, more commonly called a CT scan, can create a detailed image of the inside of the body using x-rays and computers. It is different to an x-ray because it produced a cross-sectional image of the body, similar to an MRI, making them better at looking at soft tissue and more subtle parts of the image that an x-ray may not pick up. Bones, internal organs, and blood vessels can also be seen with them. The skull, collar, back, abdomen, and sinuses are also frequently screened parts of the upper body.

3.2.2 MRI Scanners:

An MRI scan, also known as a magnetic resonance imaging scan, is a precise cross-sectional representation of a portion of the body. It's similar to a CT scan, but the image quality is better, making it possible to see tissue variations. The applications are close to those of a CT scanner: diagnosis, more information for treatment planning, and continuous treatment surveillance.

3.2.3 Ultrasound:

Ultrasound uses high-frequency waves to indicate what's going on inside a body organ. A sonogram is another name for it. Ultrasounds can generate real-time photographs of newborn children.

3.2.4 X-ray:

An x-ray is a standard technique for obtaining photographs of the interior of the body. It makes use of x-ray radiation from the electromagnetic spectrum. They are used to create images of limbs, typically to determine whether or not there are any fractures. Dentists and orthodontists use them to examine teeth as well. X-rays will also reveal bone tumors. They can be used to assist doctors during surgery. They can also be used to diagnose broken bones and determine the right recovery path.

Mostly X-rays and CT scans are also used to examine the lungs, but X-rays are favored by physicians due to their lower expense and lower radiation exposure as compared to CT scans. The figure depicts the various Medical Imaging procedures for lung and thoracic cavity visualization.

3.3 Novel Coronavirus (COVID-19)

Coronaviruses are a viral type capable of infecting and causing lung disease to people. The various spikes of the crowns on the viral surface are known as 'corona'. SARS, Middle East Respiratory Syndrome (MERS), and common cold in people are corona viruses that cause illness [59]. The World Health Organization established SARS-CoV-2 as a new coronavirus species in early 2020, following a December 2019 outbreak in China. COVID-19 was first discovered in December 2019 in Wuhan, China. Since then, the infection has spread across the globe [60].

3.3.1 Causes of COVID-19:

It's unclear what triggered it, according to researchers. Coronaviruses come in a variety of forms. They're found in bats, camels, cats, and cattle, among other species. The virus that causes COVID-19, SARS-CoV-2, is similar to MERS and SARS. They were

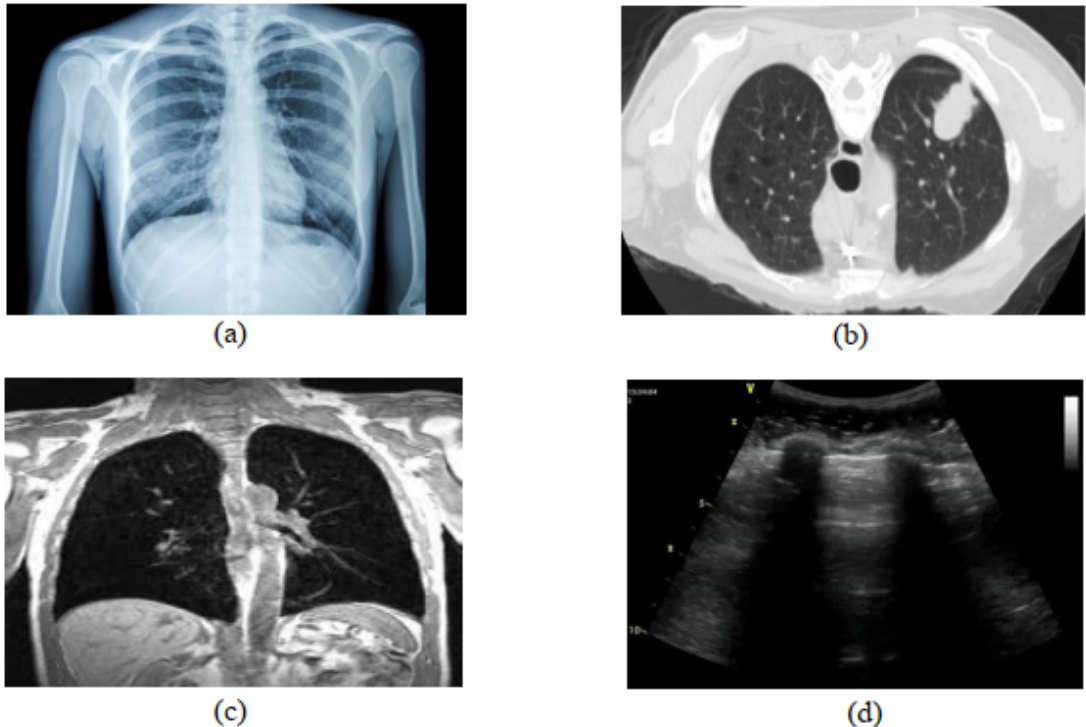


Figure 3.2: Different medical imaging for lung visualization (a) X-ray (b) CT Scan (c) MRI (d) Ultrasound

all derived from bats.

3.3.2 Risk factor:

COVID-19 will infect anybody, though the majority of infections are minor. The risk of serious illness increases as a person gets older. If someone have one of the following health conditions, they might be more susceptible to severe illness:

- Chronic kidney disease
- Chronic obstructive pulmonary disease (COPD)
- A weakened immune system because of an organ transplant
- Obesity
- Serious heart conditions such as heart failure or coronary artery disease
- Sickle cell disease
- Type 2 diabetes

CHAPTER 3: NOVEL CORONAVIRUS (COVID-19)

Conditions that could lead to severe COVID-19 illness include:

- Moderate to severe asthma
- Diseases that affect your blood vessels and blood flow to your brain
- Cystic fibrosis
- High blood pressure
- A weakened immune system because of a blood or bone marrow transplant, HIV, or medications like corticosteroids
- Dementia
- Liver disease
- Pregnancy
- Damaged or scarred lung tissue (pulmonary fibrosis)
- Smoking
- Thalassemia
- Type 1 diabetes

Any COVID-19-infected children and teenagers develop an inflammatory disorder known as multisystem inflammatory syndrome in infants, according to physicians. Doctors believe it has everything to do with the infection. It has signs that are related to toxic shock and Kawasaki disease, which induces inflammation in the blood vessels of children.

3.3.3 Symptoms of COVID-19:

The main symptoms include:

- | | | |
|-----------------------|---------------------|---------------|
| • Fever | • Trouble breathing | • Sore throat |
| • Coughing | • Body aches | • Nausea |
| • Shortness of breath | • Headache | • Diarrhea |

CHAPTER 3: NOVEL CORONAVIRUS (COVID-19)

Pneumonia, respiratory failure, cardiac disease, liver problems, septic shock, and death may also be caused by the infection. A disorder known as cytokine release syndrome or a cytokine storm can be the cause of several COVID-19 complications. This occurs after an infection causes the immune system to release inflammatory proteins such as cytokines into the bloodstream. They have the ability to destroy tissue and damage the organs.

3.3.4 COVID-19 Diagnosis:

If a person believes they have been infected and are experiencing symptoms like these, they should contact their doctor or the local health department.

- A fever of 100 degrees Fahrenheit or higher
- Coughing
- Difficulty in breathing

Testing services have become more widely accessible in most nations. Some need an appointment, whilst others are easily walk-in.

The most popular technique is a swab test. It scans the upper respiratory tract for symptoms of the infection. A swab is inserted into your nose by the person doing the procedure to get a sample from the back of your nose and mouth. The sample is normally sent to a lab where it is examined for viral content, although certain places may have accelerated testing that may have results in as few as 15 minutes.

The test is positive if there are symptoms of the infection. A negative test may indicate that the virus isn't present or that there wasn't enough to calculate. This can happen early in the course of an infection. The samples must be compiled, packed, sent to a lab, and processed, so findings normally take 24 hours.

3.3.5 Visual identification of COVID-19 in medical imaging:

Medical imaging has been used to diagnose, monitor, and aid in the care of multiple health problems for over a century including cancer, infectious diseases, heart disease, and neurological disorders. Although there are a variety of imaging procedures available,

chest X-rays, chest computed tomography (CT), and lung ultrasound are the three most often used approaches for examining COVID-19 patients.

These three methods are complementary and provide choices for determining how COVID-19 impacts various organs at various times. Since respiratory symptoms have been found to be among the first signs of COVID-19, they are used on the lung and chest region.

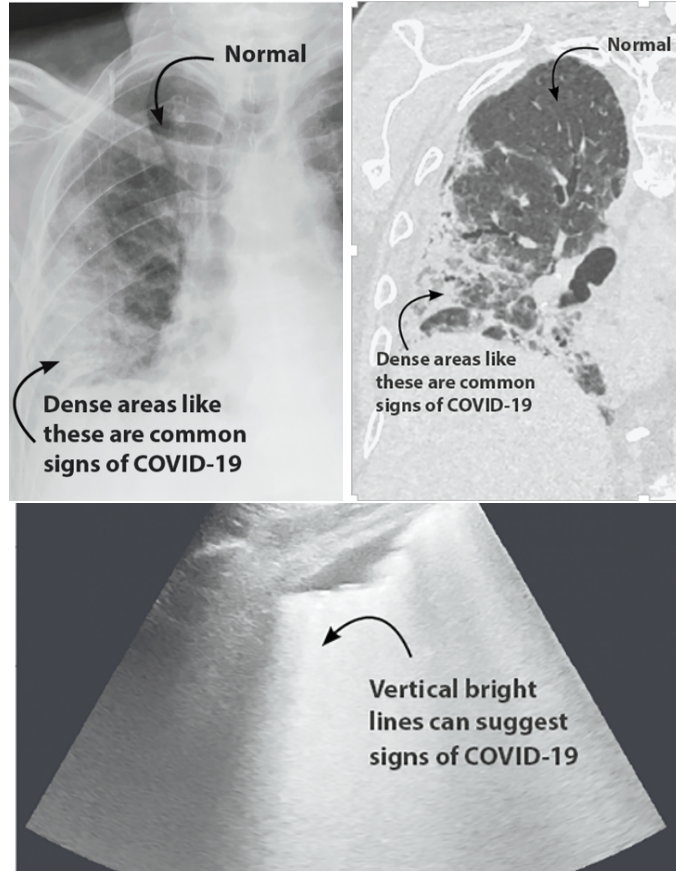


Figure 3.3: Different visual identifications for COVID-19 in medical imaging (a) X-ray
(b) CT Scan (c) Ultrasound [2]

3.3.6 Prevention:

The World Health Organization (WHO) recommends the following steps to deter the transmission of COVID-19:

- Clean your hands often. Use soap and water, or an alcohol-based hand rub.
- Maintain a safe distance from anyone who is coughing or sneezing.
- Wear a mask when physical distancing is not possible.

CHAPTER 3: NOVEL CORONAVIRUS (COVID-19)

- Don't touch your eyes, nose or mouth.
- Cover your nose and mouth with your bent elbow or a tissue when you cough or sneeze.
- Stay home if you feel unwell. If you have a fever, cough and difficulty breathing, seek medical attention.

3.3.7 Treatment:

The World Health Organization (WHO) and doctors recommend multiple treatment options for COVID-19 mentioned below:

1. Self care:

- Call your health care provider or COVID-19 hot line to find out where and when to get a test.
- Cooperate with contact-tracing procedures to stop the spread of the virus.
- If testing is not available, stay home and away from others for 14 days.
- While you are in quarantine, do not go to work, to school or to public places. Ask someone to bring you supplies.
- Keep at least a 1-metre distance from others, even from your family members.
- Wear a medical mask to protect others, including if/when you need to seek medical care.
- Clean your hands frequently.
- Stay in a separate room from other family members, and if not possible, wear a medical mask.
- Keep the room well-ventilated.
- If you share a room, place beds at least 1 meter apart.
- Monitor yourself for any symptoms for 14 days.
- Call your health care provider immediately if you have any of these danger signs: difficulty breathing, loss of speech or mobility, confusion or chest pain.
- Stay positive by keeping in touch with loved ones by phone or online, and by exercising at home.

2. Medical Treatment:

Scientists around the world are working to find and develop treatments for COVID-19.

- For chronically sick patients and others at risk of acute illness, optimal preventive treatment requires oxygen, as well as more specialized respiratory assistance, such as ventilation, for seriously ill patients.
- Dexamethasone is a corticosteroid that may help people with serious and critical illnesses spend less time on a ventilator and survive longer.

3.3.8 When to consult a doctor:

Keep indoors and watch for signs for the next 14 days if a person find that they have been exposed to someone who has tested positive for the virus or has been ill, according to UCI Health infectious disease experts.

A person should call the doctor's office if they develop the signature symptoms associated with COVID-19, including fever, shortness of breath and new cough. The doctor will decide if they need to see a doctor, be checked, go to a hospital center right away, or take care of themselves at home.

3.4 Summary:

It can be concluded that Covid-19 has evolved into a huge issue, with many people dying every day. This outbreak has affected not just a single country, but also the whole planet. Several viruses, including SARS, MERS, the flu, and many others, have received vaccines in the last decade, although they have only been used for a few days or months. Vaccines are accessible since many scientists work with viruses of this type, and only a handful have been identified. Many additional forecasts, such as plasma therapy, chest and X-ray imaging, have come into play in the meanwhile. Every day, Covid-19 steals the lives of individuals, and the disease's diagnosis is prohibitively expensive in the context of a country, state, and patients.

CHAPTER 4

Deep Learning

In recent years of computing, deep learning (DL) models in the machine learning (ML) group has been regarded as the Gold Standard. In addition, the statistical approach has increasingly become the most widely used in the field of ML, resulting in excellent findings for many dynamic cognitive functions, combining or even eliminating the human performance. The opportunity to learn huge volumes of data is one of the advantages of deep learning. Moreover, the deep learning sector has evolved rapidly and has been widely used in a wide variety of conventional applications and fields like cryptography, natural language processing, bioinformatics, robotics and control, and the medical information processing.

Therefore, this section will provide an overview of DL. We begin with a brief introduction of DL, followed by a discussion of the differences between DL and ML. We then demonstrate the circumstances that necessitate DL. Finally, we discuss the rationale for using DL.

4.1 Background of Deep Learning

DL, a subset of ML, is inspired by information processing patterns seen in the human brain. DL does not require any human-designed rules to function; rather, it leverages a huge quantity of data to map the supplied input to particular labels. DL is built with many layers of algorithms (artificial neural networks, or ANNs), each of which gives a distinct interpretation of the data supplied to it. [61, 62]

Unlike traditional ML approaches, DL can automate the learning of feature sets for a

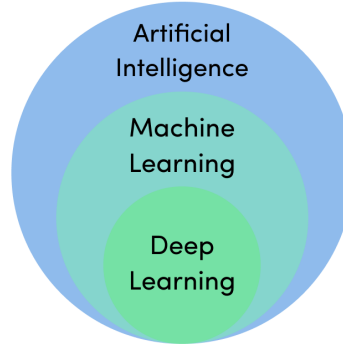


Figure 4.1: Deep Learning Family [3]

variety of purposes [61, 63]. Learning can be accomplished in a single shot with DL. Because of the tremendous development and progress of the field of big data [64, 65], DL has become an extremely popular form of ML technique in recent years. It is still being improved in terms of unique performance for various ML tasks and has eased the advancement of several learning areas such as image super-resolution, object detection, and image recognition. Recently, DL performance has surpassed human performance on tasks like image classification and image segmentation.

In 2020, DL has played an increasingly important role in the early detection of the new coronavirus (COVID-19) [66–69]. DL has become the primary technique in many hospitals across the world for automated COVID-19 classification and segmentation utilising chest X-ray & CT images & other types of imaging. We conclude this section with AI pioneer Geoffrey Hinton's remark, **"Deep learning will be able to accomplish anything."**

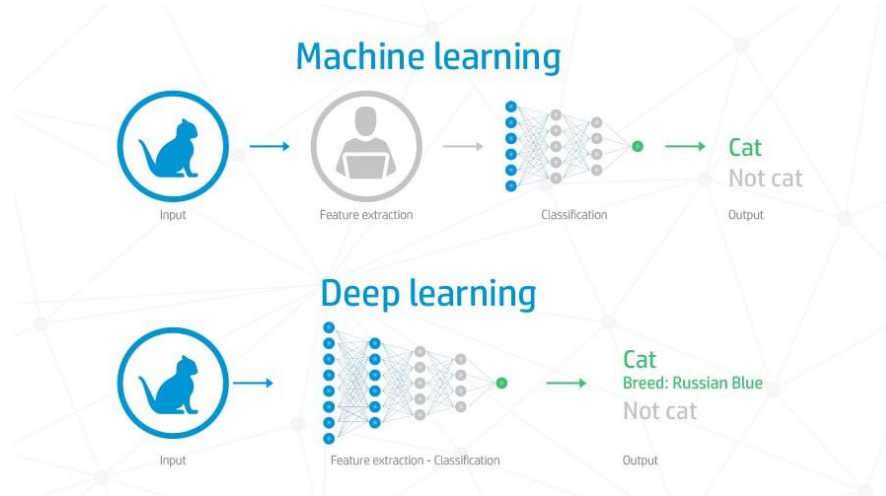


Figure 4.2: Machine Learning vs Deep Learning [4]

4.1.1 When to apply DL:

Machine learning is useful in many situations, and in certain cases, it is as good as or better than human specialists, implying that DL might be a solution in situations when human experts are unavailable or situations in which humans are unable to explain judgments taken in the course of their expertise. Furthermore, DL can be a solution to a problem where the solution to the problem changes over time, or where the solution requires adaption based on individual situations.

4.1.2 Why Deep Learning:

Deep Learning approaches outperform others when there is a dearth of domain expertise for feature introspection since you have to worry less about feature engineering. Deep Learning excels at difficult tasks like image classification, natural language processing, and speech recognition. Several performance measures like "universal learning approach, robustness, generalization & scalability" may answer this question.

4.1.3 Classification of Deep Learning approaches:

There are three types of DL approaches: unsupervised, partially supervised (semi-supervised), and supervised. Furthermore, deep reinforcement learning (DRL), often known as RL, is another form of learning approach that is generally classified as partially supervised (and occasionally unsupervised) learning.

4.1.4 Types of Deep Learning networks:

The most well-known deep learning networks are recursive neural networks (RvNNs), RNNs, and CNNs. Because of the relevance of CNN's, they are thoroughly described. Furthermore, it is the most broadly utilized network in a variety of applications.

4.2 Convolutional Neural Network

The CNN algorithm is the most well-known and widely used in the field of deep learning [70]. The major advantage of CNN over its predecessors is that it automatically identifies important characteristics without the need for human intervention. CNNs have been

widely used in a variety of disciplines, including computer vision, speech processing, face recognition, and so on. CNNs, like traditional neural networks, were inspired by neurons in human and animal brains.

A popular type of CNN, comparable to the multi-layer perceptron (MLP), consists of several convolution layers following sub-sampling (pooling) layers, with FC layers at the end. Figure 4.3 is an example of CNN architecture for image categorization.

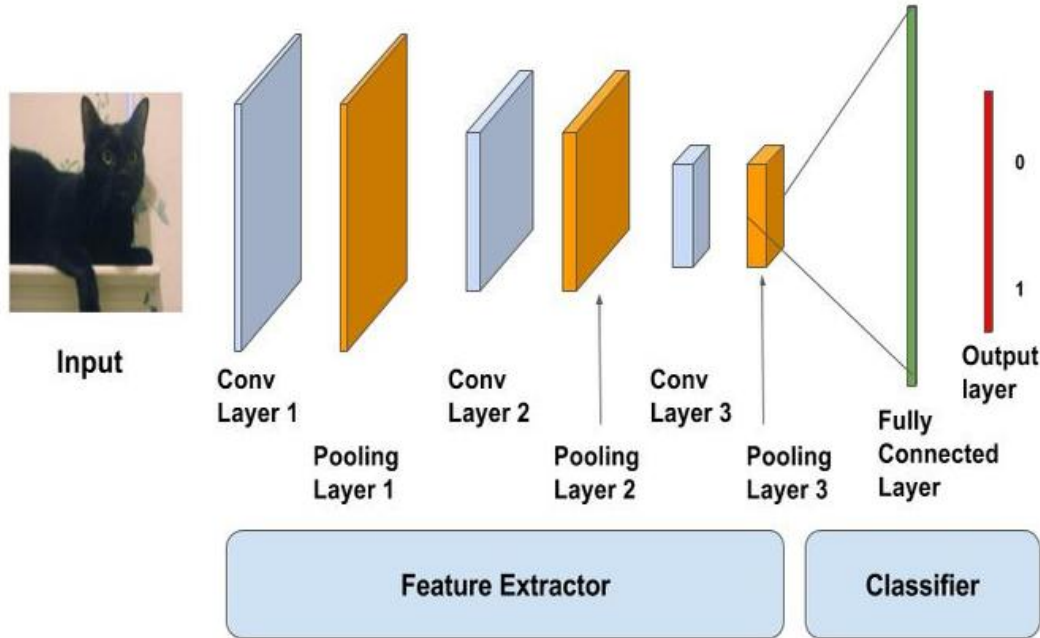


Figure 4.3: CNN Architecture for Image Classification [5]

4.2.1 The advantages of using CNN:

The primary rationale for considering CNN is the weight sharing feature, which minimises the amount of trainable network parameters, allowing the network to improve generalisation and avoid overfitting. Moreover, CNN makes large-scale network deployment considerably easier than other neural networks.

4.2.2 CNN Layers:

The CNN architecture is made up of several levels (or so-called multi-building blocks). Each layer of the CNN design is covered in detail below, including its purpose:

Convolutional Layer: Convolutional layers are the layers in a deep CNN where filters are applied to the original image or other feature maps. The majority of the network's user-specified parameters are located here. The number of kernels and the size of the kernels are the most significant factors.

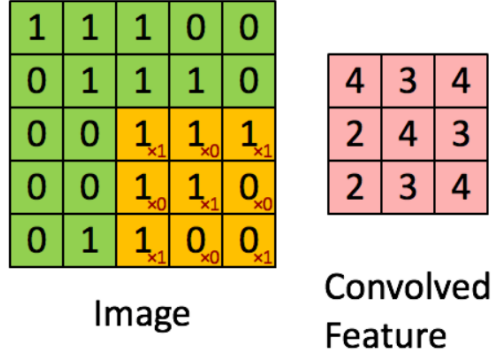


Figure 4.4: Convolutional Layer [6]

Pooling Layer: A pooling layer is another component of a CNN. Its purpose is to gradually lower the spatial dimension of the representation in order to reduce the number of parameters and computation in the network. The pooling layer acts independently on each feature map. The most popular method for pooling is max pooling.

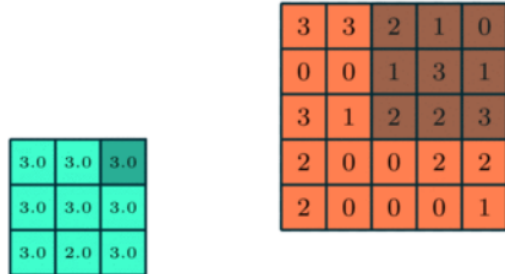


Figure 4.5: Pooling Layer [7]

Activation Function: The activation function is a node placed at the end of or between Neural Networks. They aid in determining whether or not the neuron will fire. The activation function is the nonlinear modification applied to the input signal. This modified output is subsequently given as input to the next layer of neurons. "Sigmoid, Tanh, ReLU, Leaky ReLU" are the most frequent kinds of activation functions used in

CNN and other deep neural networks.

Fully Connected Layer: Fully Connected Layer is simply, feed forward neural networks. Fully Connected Layers form the last few layers in the network. The input to the fully connected layer is the output from the final Pooling or Convolutional Layer, which is flattened and then fed into the fully connected layer.

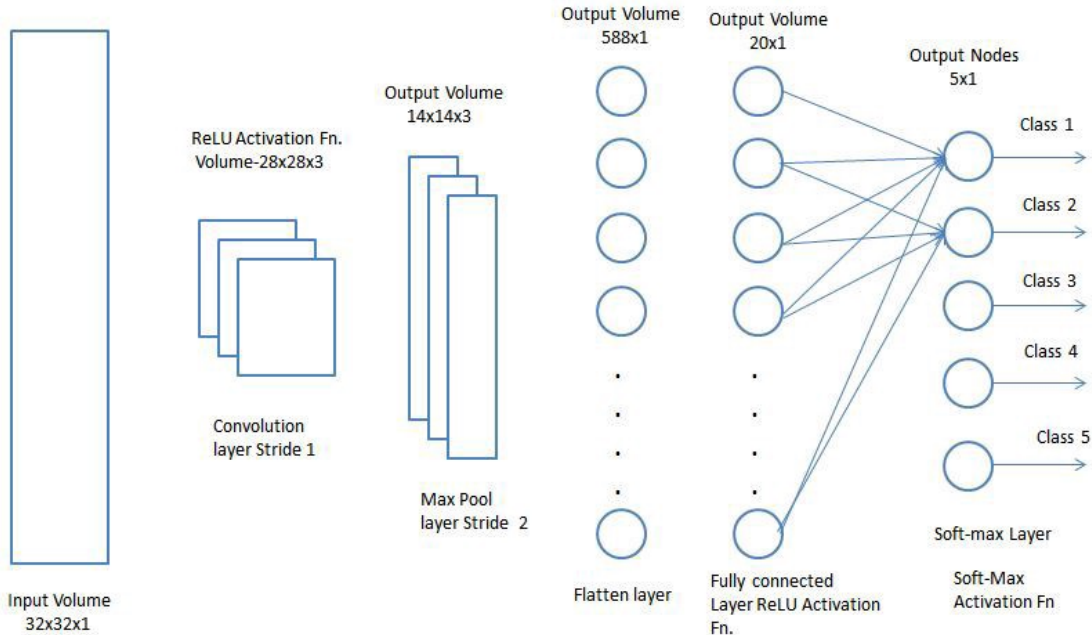


Figure 4.6: Fully Connected Layer [8]

Loss Function: In the CNN model, certain loss functions are used in the output layer to compute the expected error generated throughout the training data. This error indicates the discrepancy between the actual and expected output. Softmax loss function, Euclidean Loss Function & Hinge Loss Function etc are some various forms of loss functions that are used in various issue categories.

Regularization: Regularization is one method for preventing overfitting & for controlling model complexity. If there are a lot of features, there will be a lot of weights, making the model prone to overfitting. As a result, regularisation lessens the strain on these weights. To minimise over-fitting, several intuitive ideas including as dropout, drop weights, batch normalization, data augmentation, and so on are employed to aid regularization.

Optimizer Selection: Optimizer are techniques or approaches that are used to modify the characteristics of the neural network, such as weights and learning rate, in order to minimize the loss. Optimizer aid in obtaining outcomes more quickly. Batch gradient descent, adagrad, adadelta, Adam etc are some examples of optimizers used in CNN.

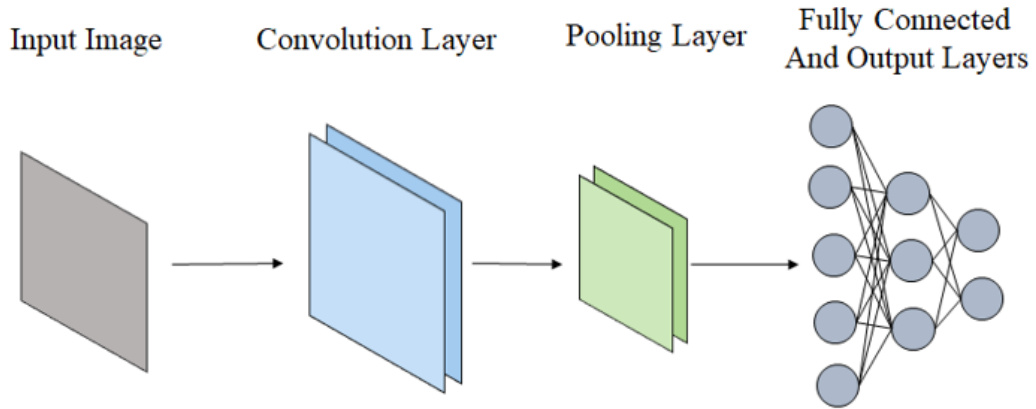


Figure 4.7: An example of layered architecture of a basic convolutional neural network [9]

4.3 CNN Architectures

Several CNN architectures have been introduced over the previous ten years. Model architecture is an important component in enhancing the performance of many applications. From 1989 until the present, several changes have been made to the CNN architecture. Modifications such as structural reformulation, regularization, parameter optimizations, and so on are examples of such changes. On the other hand, it should be emphasized that the significant improvement in CNN performance was primarily attributable to processing-unit rearrangement as well as the invention of innovative blocks. The most innovative advancements in CNN designs, in particular is focused on the utilization of network depth. In this section, we will look at the most common CNN architectures for classification & segmentation.

4.3.1 CNN Architectures for Classification:

VGG Net: Simonyan and Zisserman presented the VGG network architecture in their 2014 publication, Very Deep Convolutional Networks for Large Scale Image Recognition [71]. This network is distinguished by its simplicity, since it employs just 3x3 convolutional layers stacked on top of each other in increasing depth. Max pooling handles volume size reduction. After that, two fully-connected layers with 4,096 nodes each are followed by a softmax classifier.

Simonyan and Zisserman found training VGG16 and VGG19 difficult, so they proceeded by training smaller versions of VGG with fewer weight layers. VGGNet, unfortunately, has two main drawbacks:

- Training is very slow.
- The weights of the network design are relatively substantial (in terms of disk/bandwidth).

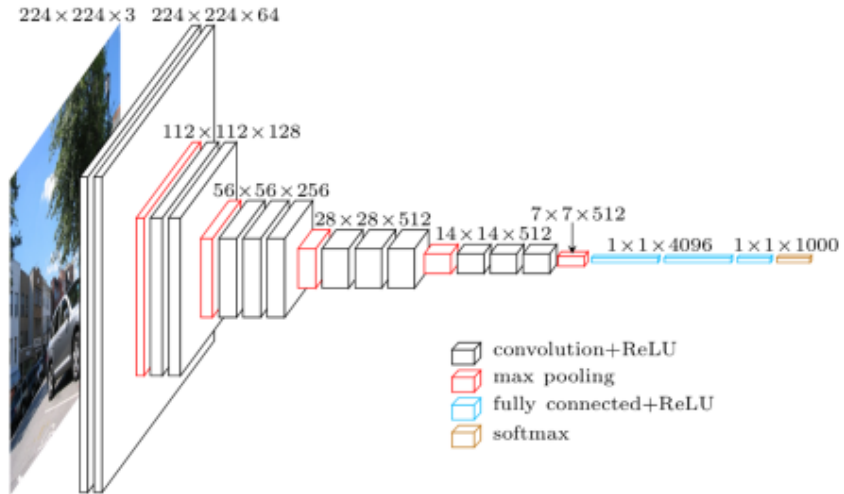


Figure 4.8: VGG architecture [10]

Densenet: DenseNet is one of the most recent neural network breakthroughs for visual object detection. DenseNet is quite similar to ResNet, with a few key changes. DenseNet concatenates the output of the previous layer with the output of the future layer. DenseNet was created particularly to improve the vanishing gradient-induced reduction in accuracy in high-level neural networks. In plain terms, the information disappears before reaching its destination due to the longer path between the input layer and the output layer.

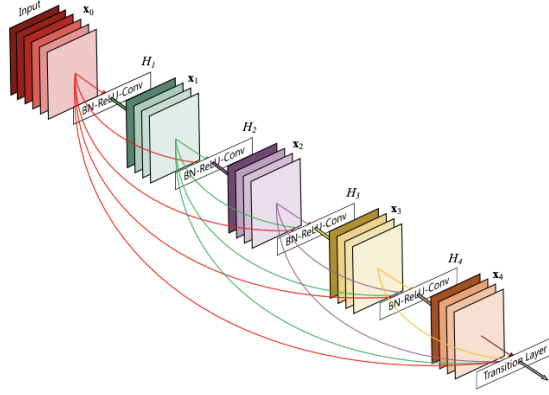


Figure 4.9: The Densenet Architecture [11]

Resnet: ResNet, 'in contrast to typical sequential network architectures such as Alex Net, VGG" is a type of exotic architecture that relies on micro-architecture modules also known as network-in-network architecture.

The term "micro-architecture" refers to the collection of "building blocks" utilized to form the network. The macro-architecture is constructed from a set of micro-architecture building pieces (along with your standard CONV, POOL, and so on) (i.e.,. the end network itself).

First introduced by He et al. in their 2015 paper *Deep Residual Learning for Image Recognition* [72], ResNet is much deeper than VGG16 and VGG19. The model size is significantly less owing to the use of global average pooling rather than fully-connected layers.

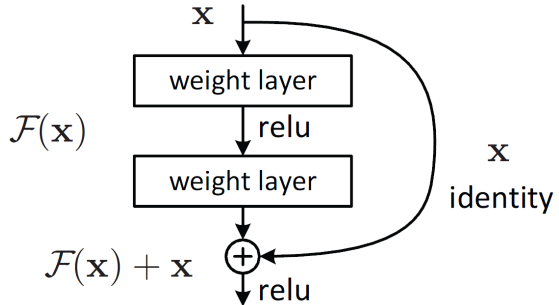


Figure 4.10: Block Diagram of Resnet [12]

Mobile Net: MobileNet is a form of convolutional neural network that is intended for use in mobile and embedded vision applications. They are based on a simplified design that use depth wise separable convolutions to construct lightweight deep neural

networks with minimal latency for mobile and embedded devices. The MobileNet layers' purpose is to transform the pixels in the input image into features that characterize the image's contents and pass them along to the other layers. As a result, MobileNet is utilized as a feature extractor for a second neural network in this case.

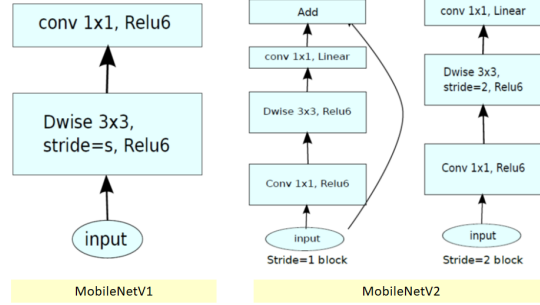


Figure 4.11: Architecture of Mobile net V1 & V2 [13]

Xception: Xception was proposed by François Chollet [73], the developer and primary maintainer of the Keras library. Xception is an Inception architectural modification that replaces conventional Inception modules with depth wise separable convolutions.

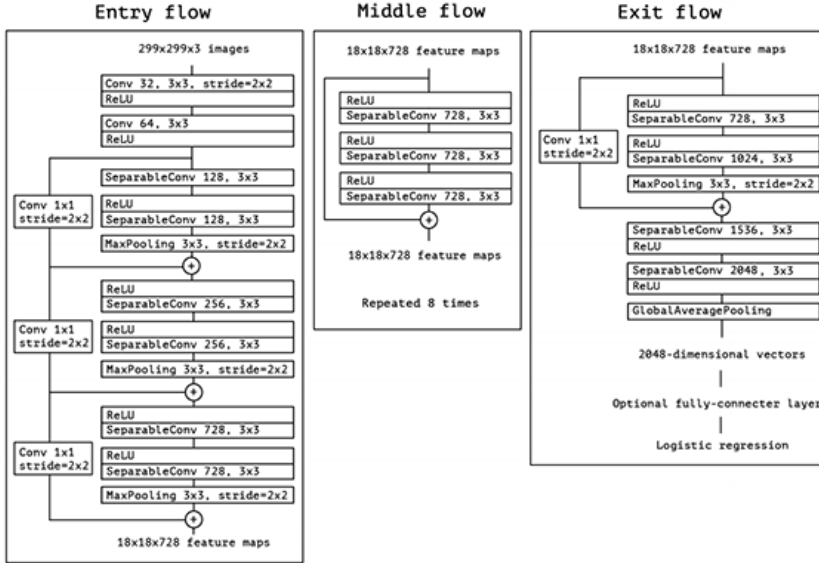


Figure 4.12: The Xception Architecture [14]

Inception(Resnet & V3/4): As improved versions of Inception-V1/2, Szegedy et al. [74] suggested Inception-ResNet and Inception-V3/4. The idea was to reduce computing costs while maintaining greater network generalisation. As a result, Szegedy et al.

chose asymmetric small-size filters over large-size filters. Furthermore, previous using the large-size filters, they used a bottleneck of 1x1 convolution. Because of these modifications, the functioning of conventional convolution is quite similar to cross-channel correlation.

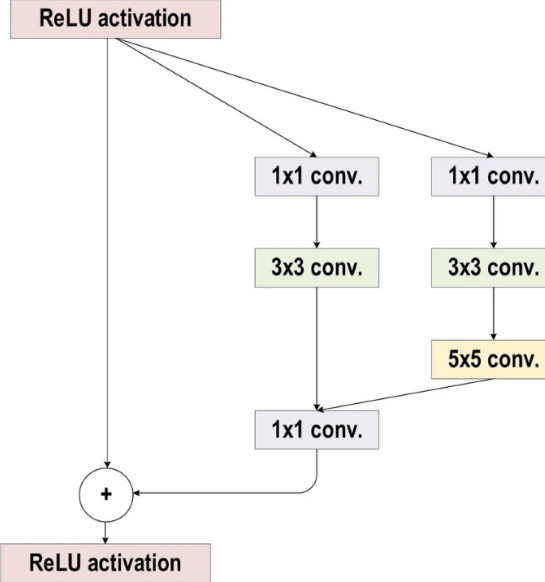


Figure 4.13: The Inception Resnet Architecture [15]

EfficientNet: EfficientNet is a convolutional neural network architecture and scaling approach that uses a compound coefficient to equally scale all depth/width/resolution dimensions. EfficientNet use a compound coefficient to evenly scale network breadth, depth, and resolution.

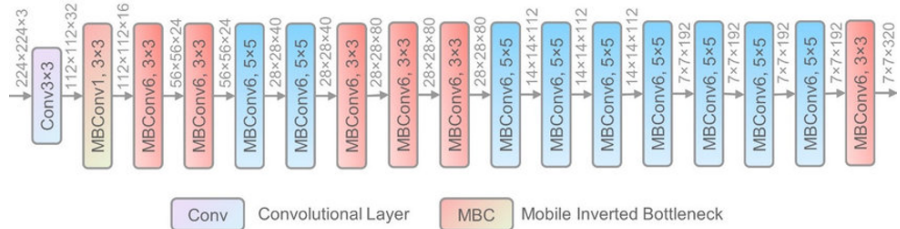


Figure 4.14: The Efficientnet Architecture [16]

Nasnet: Nasnet is a CNN architecture that searches for the best algorithm to do the best on a specific job. Nasnet has been used to build networks that outperform hand-coded systems. NAS methods are categorised according to the search space, search technique, and performance estimation strategy used.

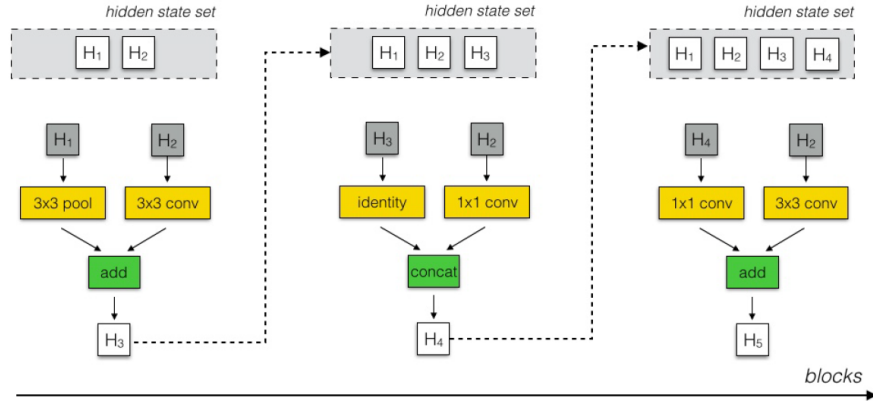


Figure 4.15: Schematic diagram of the NASNet Architecture [17]

4.3.2 CNN Architectures for Segmentation:

Unet: U-Net is a convolutional neural network that was designed to segment biological pictures. When imagined, its architecture resembles the letter U, therefore the name U-Net. Its architecture is divided into two parts: the left portion, which is the contracting path, and the right part, which is the expansive path. The contracting path's role is to capture context, whereas the expanding path's role is to help in accurate localization.

Two three-by-three convolutions make up the contracting path. Following the convolutions is a rectified linear unit and a two-by-two max-pooling computation for down sampling.

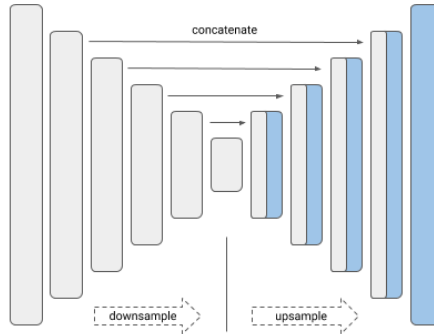


Figure 4.16: The Unet Architecture [18]

Feature Pyramid Network (FPN): Another comparable design is Feature Pyramid Network (FPN), however, instead of copying and attaching features like in Unet, FPN

applies a 1×1 convolution layer and adds the features to it.

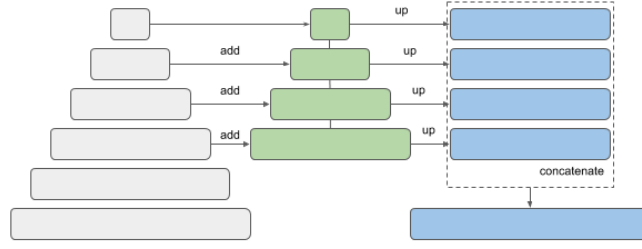


Figure 4.17: The FPN Architecture [18]

Pyramid Scene Parsing Network (PSPNet): PSPNet, or Pyramid Scene Parsing Network, is a semantic segmentation approach that uses a pyramid parsing module to leverage global context information via context aggregation depending on various regions. The combination of local and global cues strengthens the ultimate prediction.

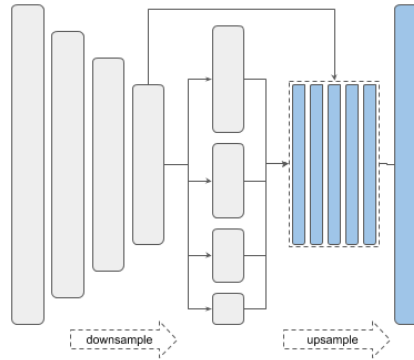


Figure 4.18: The PSPNet Architecture [18]

Link Net: Linknet is a deep neural network architecture that is developed for semantic segmentation. It can provide real-time performance on both GPU's and embedded devices. Members of Purdue University's e-Lab designed this network. Linknet can process an input image with a resolution of 1280x720 at a rate of 2 frames per second and 19 frames per second, respectively. After each down sampling block, the Linknet architecture attempts to efficiently exchange the knowledge learned by the encoder with

the decoder. This outperforms utilizing pooling indices in the decoder or simply employing fully convolutional networks in the decoder. This feature forwarding approach not only provides with high accuracy values, but it also allows us to have only a few parameters in our decoder.

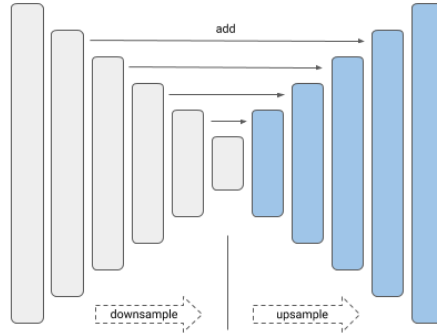


Figure 4.19: The LinkNet Architecture [18]

4.4 Applications of Deep Learning

Currently, numerous DL applications are being used all over the world. Healthcare, social network analysis, audio and speech processing (such as recognition and enhancement), visual data processing methods (such as multimedia data analysis and computer vision), and NLP (translation and sentence classification) are examples of these applications. These applications are divided into five categories: classification, localization, detection, segmentation, and registration. Although each of these activities has its own objective, as seen in Fig.20, there is significant overlap in the pipeline implementation of these applications.

Healthcare is one of the most significant and diverse DL applications. Because of its relevance to human lives, this field of study is essential. Furthermore, DL has demonstrated exceptional performance in healthcare.

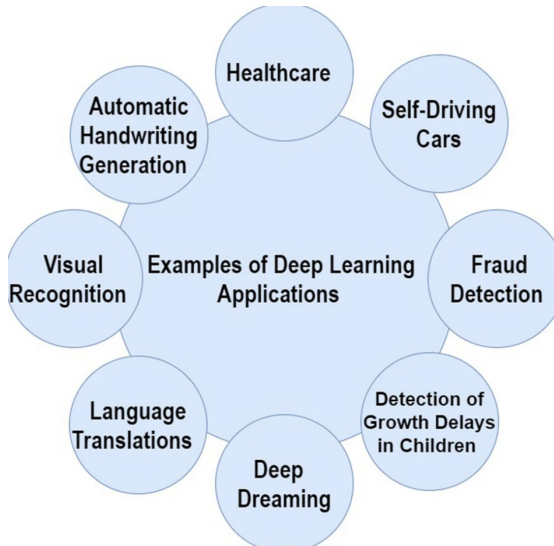


Figure 4.20: Example of DL Applications [19]

4.5 Evaluation Metrics

The evaluation metrics used in DL activities are critical to getting optimal outcomes. The following are some of the most well-known evaluation metrics.

Accuracy: Calculates the ratio of correct predicted classes to the total number of samples evaluated.

Recall: Utilized to calculate the fraction of positive patterns that are correctly classified.

Precision: Utilized to calculate the fraction of negative patterns that are correctly classified

F1-Score: Calculates the harmonic average between recall and precision rates.

Jaccard Index: Jaccard index, also known as the Jaccard similarity coefficient, is a statistic used for gauging the similarity and diversity of sample sets.

$$\text{Recall} = \frac{TP}{TP + FN} \quad (4.5.1)$$

$$\text{Precision} = \frac{TN}{TN + FP} \quad (4.5.2)$$

$$\text{Accuracy} = \frac{TP + TN}{TP + TN + FP + FN} \quad (4.5.3)$$

$$\text{Jaccard Index} = \frac{TP}{TP + FP + FN} \quad (4.5.4)$$

$$\text{F1Score} = \frac{2TP}{2TP + FP + FN} \quad (4.5.5)$$

4.6 Summary

AI's continual advancement opens up new avenues for machine development. Deep Learning vs Machine Learning are considered subsets of Artificial Intelligence. Both Machine Learning and Deep Learning are unique algorithms that can execute certain jobs, each with its own set of benefits. Machine Learning algorithms are capable of evaluating and learning from supplied data, and are ready to make a final choice with the aid of a human assistant, but deep learning does not require as much assistance due to fundamental replication of human brain process and comprehension of the context .

The article, titled "**Deep Learning for AI**" envisions a future in which deep learning models can learn with little or no human assistance, are adaptable to changes in their environment, and can handle a wide range of reflexive and cognitive issues.

CHAPTER 5

Methodology

In this chapter, the proposed classification and segmentation approach for the automatic analysis of COVID-19 disease in CT and X-ray images is provided. Moreover, a brief details of the datasets is also being discussed in this chapter. We will begin with the datasets and then to the proposed classification and segmentation techniques.

Also, some transfer learning concepts, implementation details, performance evaluation metrics and the strategy for implementing the models for classification and segmentation.

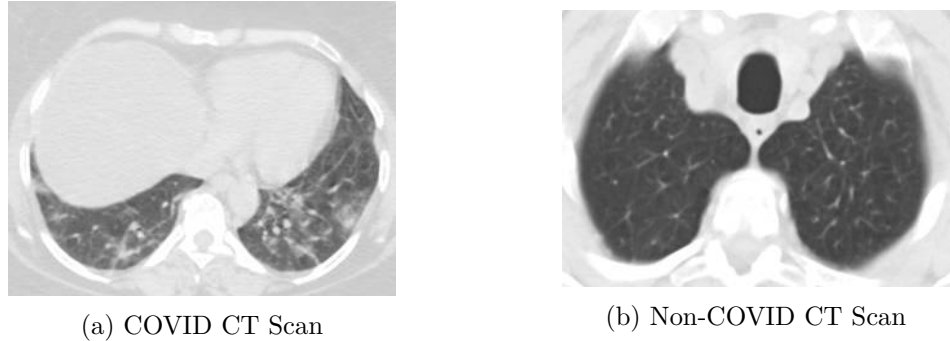
5.1 Databases

The proposed methodology is evaluated using freely available classification and segmentation datasets.

5.1.1 Classification Datasets:

SARS COV II CT Scan Dataset: The first dataset build by Eduardo Soares et al called the SARS-CoV-2 CT scan dataset [20] contains 1252 CT scans that are positive for SARS-CoV-2 infection (COVID-19) and 1229 CT scans for patients non-infected by SARS-CoV-2, 2481 CT scans in total. These data have been collected from real patients in hospitals from Sao Paulo, Brazil.

COVID CT Dataset (GitHub): Xingyi Yang [21] et al presented a database of CT images including 349 CT scans of COVID-19 positive cases of 216 patients and 195 non-COVID-19 CT scans.



(a) COVID CT Scan (b) Non-COVID CT Scan

Figure 5.1: CT Scans of SARS COV II Dataset [20]

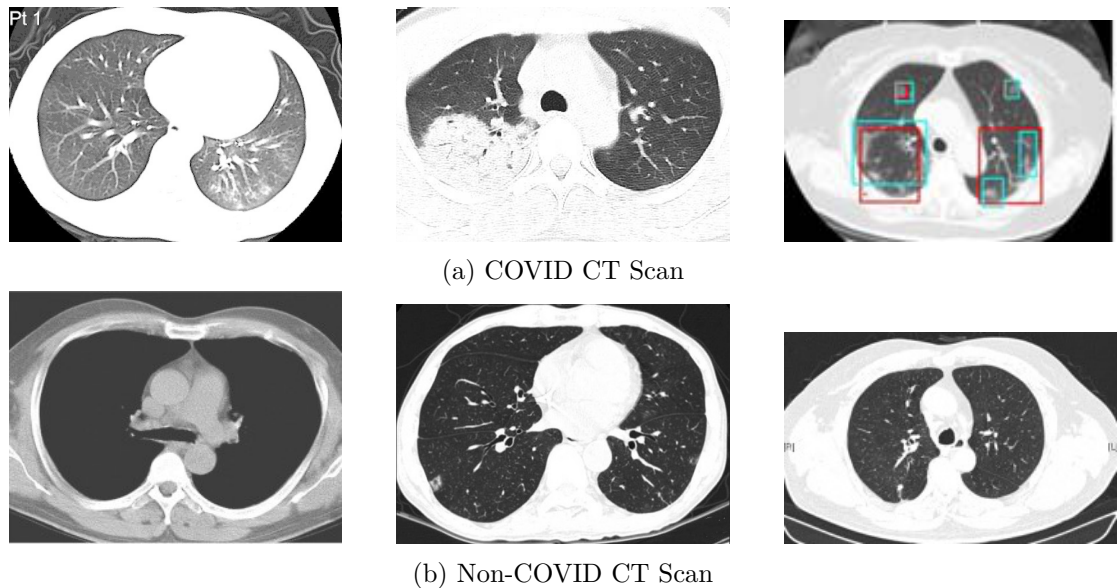


Figure 5.2: CT Scans of COVID CT Dataset [21]

COVID-19 Radiography X-ray Database (Kaggle): A collaborative efforts with medical doctors, group of researchers from University of Dhaka & Qatar University as well as some other associates from Malaysia & Pakistan created a database of chest X-ray images for COVID-19 positive cases, normal and viral pneumonia images [22, 23]. There are 3616 COVID-19 positive images, 10.2k normal images & 1345 Pneumonia images in their current release and continuing to update this database as soon as new X-ray images for COVID-19 patients becomes available.

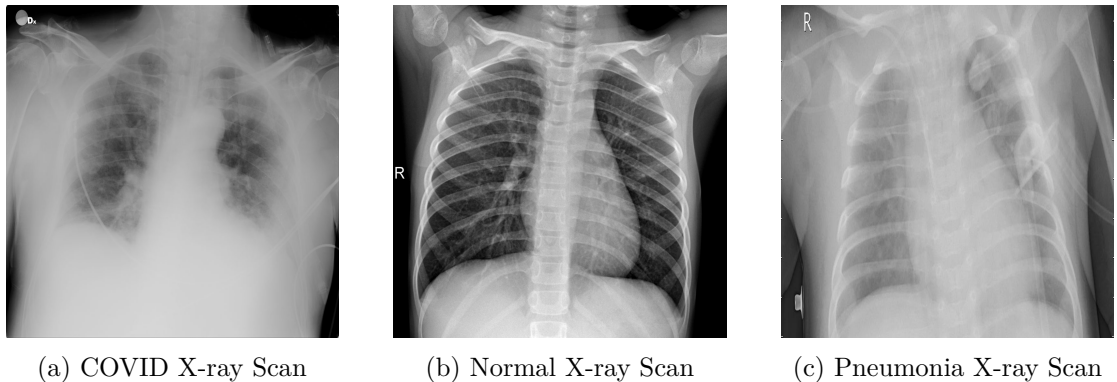


Figure 5.3: X-ray Scans of COVID Radiography Dataset [22, 23]

Joseph Paul Cohen COVID X-ray Dataset:

Joseph Paul Cohen et al introduced first public COVID-19 X-ray image database [24]. This dataset presently comprises hundreds of frontal view X-rays and is the broadest public asset for COVID-19 image and prognostic data, making it an important resource for developing & evaluating technologies that can help in the diagnosis of COVID-19. There are 435 COVID and 505 Non-COVID chest X-ray images from 412 people from 26 nations in their current release and this number is expanding.

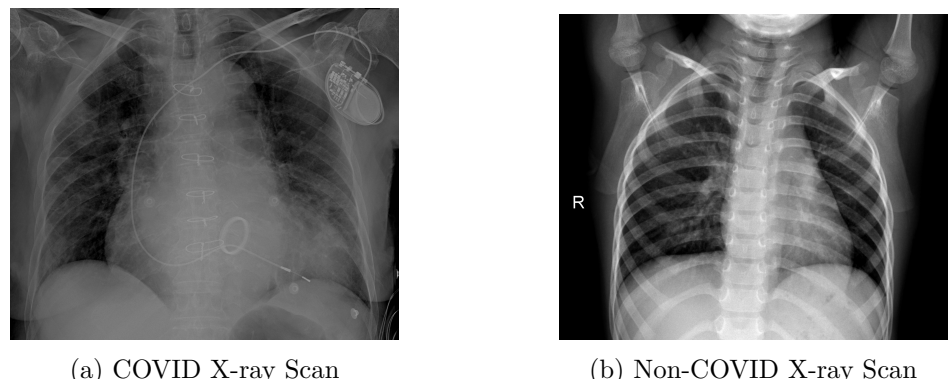


Figure 5.4: X-ray Scans of COVID IEEE-8023 Dataset [24]

Table 5.1: Overview of the Classification Datasets

Classification Method	Number of Samples	Links
Binary Class	2481 CT Scans	https://www.kaggle.com/plameneduardo/sarscov2-ctscan-dataset [20]
Binary Class	544 CT Scans	https://github.com/UCSD-AI4H/COVID-CT [21]
Binary Class	940 X-ray Scans	https://github.com/ieee8023/covid-chestxray-dataset [24]
Multi Class	15153 X-ray Scans	https://www.kaggle.com/tawsifurrahman/covid19-radiography-database/data [22, 23]

5.1.2 Segmentation Datasets:

Medical Segmentation: This dataset consists of two parts "Radiopedia and MedSeg". The Medseg part consists of 100 axial CT images from 40 patients with COVID-19 that were converted from openly accessible JPG images [25]. The conversion process is described in detail in the following blog post: "*Covid-19 radiology data collection and preparation for Artificial Intelligence*". The images were segmented by a radiologist using 3 labels: ground-glass, consolidation, lungs. Ground glass opacity (GGO) refers to the hazy grey regions that may be seen in lungs CT scans or X-rays. The grey patches represent increased density throughout the lungs. Lung consolidation is when the air that normally fills the tiny airways in the lungs gets replaced with something else. Depending on the reason, the air may be replaced by a fluid such as pus, blood, or water, a solid such as stomach contents or cells.

The radiopedia part includes a dataset consisting of whole volumes of both positive & negative slices, 373 out of the total of 829 slices have been evaluated by a radiologist as positive and segmented.

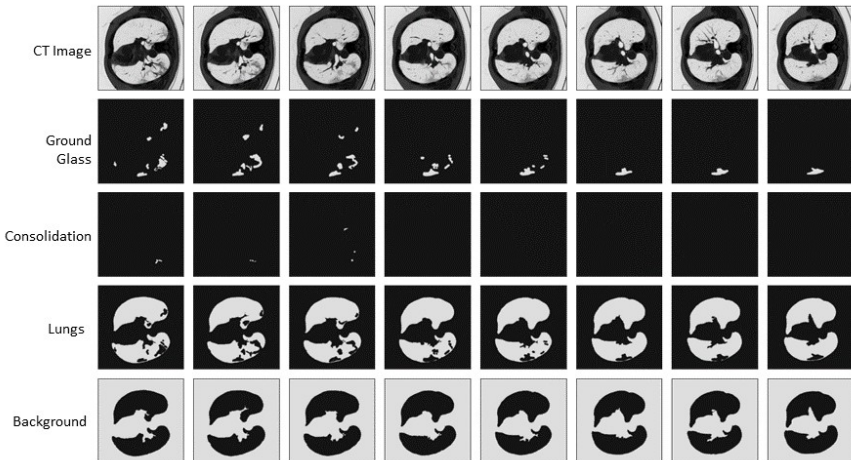


Figure 5.5: Visual Appearance of Medical Segmentation Dataset with Masks [25]

COVID-19 CT Lung & Infection Dataset (Zenodo): The second dataset contains 20 CT scans of patients diagnosed with COVID-19 as well as segmentation of lungs and infections made by experts. The images were segmented by a radiologist using 3 labels: “Lung mask, Infection mask, Lung + Infection mask” [26].

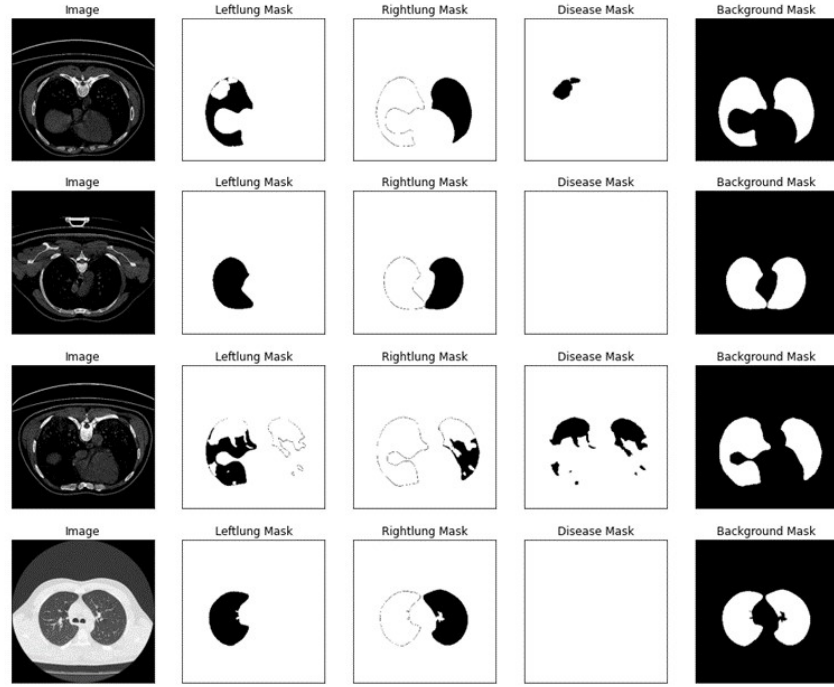


Figure 5.6: Visual Appearance of Zenodo Dataset with Masks [26]

Table 5.2: Overview of the Segmentation Datasets

Segmentation Method	Number of Samples	Links
<i>Binary & Multi-Class</i>	20 CT Scans	https://zenodo.org/record/3757476#.YUG_UMvivIV [26]
<i>Multi-Class</i>	100 CT Scans from 40 patients	http://medicalsegmentation.com/covid19/ [25]
<i>Multi-Class</i>	829 slices from 9 patients	http://medicalsegmentation.com/covid19/ [25]

5.2 Proposed Architecture for Classification

As discussed earlier, the proposed classification model will segregate COVID-19 CT & X-ray images from healthy images by performing classification.

The CNN architectures used for feature extraction purpose are mentioned below with variants shown in parenthesis. Details are discussed in chapter 4.

CHAPTER 5: METHODOLOGY

- VGG (16,19)
- Densenet (121)
- Nasnet (Large)
- Efficientnet (B0)
- Mobilenet (V2)
- Resnet (50, 50V2, 101V2)
- Xception
- Inception (Resnet V2, V3)

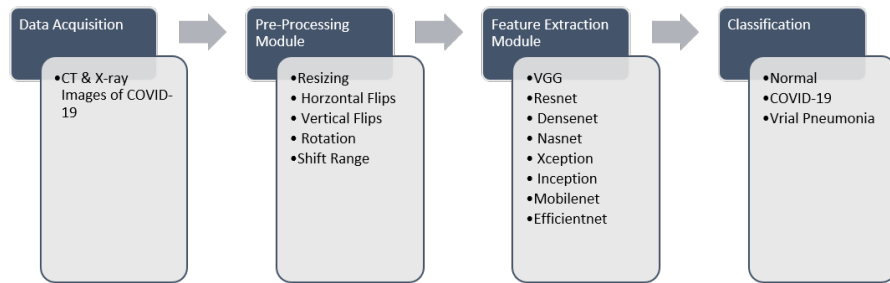


Figure 5.7: Workflow of COVID-19 Classification

5.2.1 Proposed Architecture:

In our study, we applied deep CNN architectures on binary & multi-class classification & choose the COVID-19 as the target concept to evaluate how the classification model make predictions of COVID-19 cases.

The block diagrams for training & testing of the proposed architecture are shown in figure below:

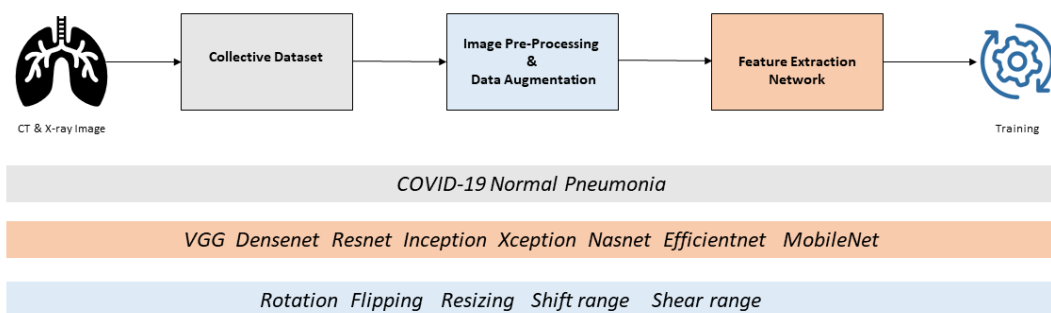


Figure 5.8: Block Diagram for Training

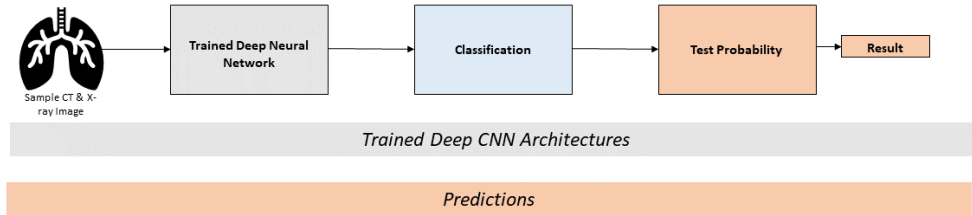


Figure 5.9: Block Diagram for Testing

5.2.2 Transfer Learning:

Transfer learning is a machine learning approach in which a previously trained model is utilised as the foundation for a new model and task. It can not only reduce the need for the work required to acquire training data, but it can also speed up the training process.

To leverage transfer learning on deep convolutional neural networks, two frequently used methods are used. The first method is feature extraction, in which the pretrained model is simply utilised to extract image features for the input of the new classification model while maintaining both its initial architecture and the learnt parameters. The second method modifies the pretrained model, such as architectural changes and parameter tuning, in order to improve extracted image features on the new dataset and obtain optimal results.

The first method is employed in this study. Moreover, to pretrain CNN architectures, we leverage ImageNet, a large-scale dataset comprising of 1.2 million high-resolution images in 1,000 distinct classes (e.g., fish, bird, tree, flowers, sport, room, etc.).

5.2.3 Data Augmentation:

The amount of data available often enhances the performance of deep learning neural networks. Data augmentation is a method of artificially creating fresh training data

from existing data. This refers to changes of the training set images that the model is inclined to consider.

Multiple libraries are available for data augmentation in Python. PIL and Augmentor are two libraries that can operate on images directly. Augmentor also has a pipelining feature that allows us to work on many images at once. Apart from keras preprocessing, we used ImageDataGenerator. Rotation, cropping, zooming, colour range modifications, grayscaling, and flipping are examples of image augmentations.

Data augmentation can be divided into two groups. The first is image transformation, while the second is the creation of synthetic images. We used transformation data augmentation technique for the classification problem. The techniques for data augmentation used for classification are listed in the table below.

Table 5.3: Data Augmentation for Classification

Augmentation	Probability
Rotation	20
Flipping	Horizontal
Resizing	True
Shift Range	0.2
Shear Range	0.2
Zoom Range	0.2

5.2.4 Model Hyperparameters:

The following hyperparameters are used for training:

Binary Classification Model: Image size = 224x224, Batch size = 32, cross entropy loss, Adam optimizer with learning rate = 0.0001, 20 epochs in total with early stopping.

Multi Classification Model: Image size = 240x240, Batch size = 32, cross entropy loss, Adam optimizer with learning rate = 0.0001, 50 epochs in total with early stopping.

5.2.5 Evaluation Metrics:

The model's performance is evaluated using five evaluation metrics: accuracy, confusion matrix, precision, recall, and F1-score.

Confusion Matrix: On a classification issue, a confusion matrix provides a summary of anticipated and true labels. It provides information not just about the mistakes but also on the sorts of errors made by the classifier. Figure 5.2 depicts the confusion matrix schema in a binary classification problem.

		True Class	
		Positive	Negative
Predicted Class	Positive	TP	FP
	Negative	FN	TN

Figure 5.10: Schema of confusion matrix [27]

Based on the confusion matrix, the accuracy, precision, recall, and F1-score can be calculated using the formulas mentioned below:

$$\text{Accuracy} = \frac{TP + TN}{TP + TN + FP + FN} \quad (5.2.1)$$

$$\text{Precision} = \frac{TN}{TN + FP} \quad (5.2.2)$$

$$\text{Recall} = \frac{TP}{TP + FN} \quad (5.2.3)$$

$$\text{F1Score} = \frac{2TP}{2TP + FP + FN} \quad (5.2.4)$$

5.3 Proposed Architecture for Segmentation

The aim of segmentation is to extract from the image the region of interest. In our situation, the area of the lung affected by the coronavirus and the lungs in CT images.

The architectures used for the COVID-19 semantic segmentation are mentioned below with backbones used.

Architectures:

- Unet
- Link Net
- Pyramid Scene Parsing Network (PSPNet)
- Feature Pyramid Network (FPN)

Backbones

- VGG-19
- Densenet 121
- Seresnext 101
- Inception Resnet V2
- Efficientnet B3
- Mobilenet V2

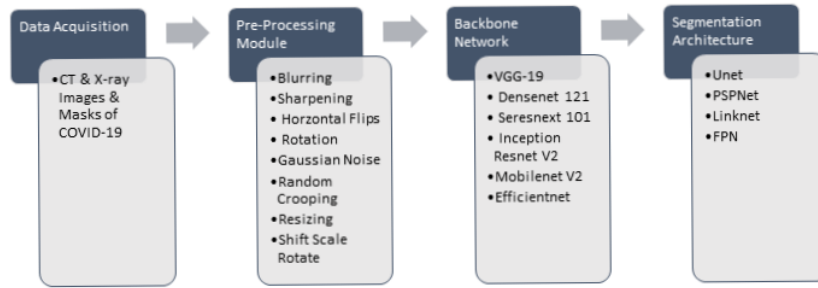


Figure 5.11: Workflow of COVID-19 Segmentation

5.3.1 Proposed Architecture:

Our segmentation problem is a binary & multi-class problem. So we have two classes for binary class & four classes for multi-class. The details of the classes are shown in the table 5.2.

The block diagram for training & testing of the proposed architecture are shown in Fig 5.12 and 5.13 respectively:

Table 5.4: Segmentation Masks

Class	Segmentation Masks
<i>Binary Class</i>	Disease
	Background
<i>Multi Class</i>	Ground Glass
	Consolidation
	Lungs
	Background
<i>Multi Class</i>	Disease
	Left Lung
	Right Lung
	Background

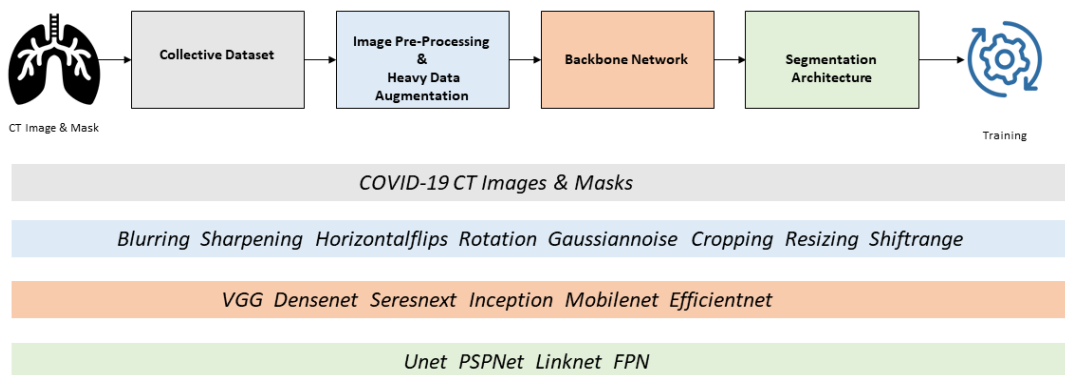


Figure 5.12: Block Diagram for Training

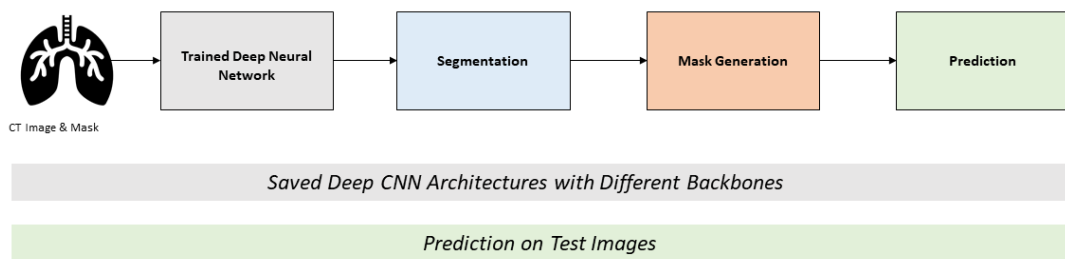


Figure 5.13: Block Diagram for Testing

5.3.2 Data Augmentation:

The availability of annotated training data is frequently a constraint in medical image segmentation. 'Data augmentation' prevents the network from memorising training data and improves its performance on data outside of the training set. As a result, it is critical in the development of effective deep learning pipelines.

Due to limited number of COVID CT segmented image and masks, data augmentation using the synthetic image creation theme was utilized. Using the "albumentation library" on binary & multi-class segmentation, resizing, horizontal flips, shift scale rotate, cropping, Gaussian noise and perspective augmentation have been utilized for best results. Table below shows the applied augmentation techniques with probabilities.

Table 5.5: Data Augmentation for Segmentation

Augmentation Technique	Probability
Random Crop	True
Flipping	Horizontal (0.5)
Resizing	True
Shift	0.1
Scale	0.5
Rotate	0
Gaussian Noise	0.2
Blurring	0.1
Sharpening	0.1

5.3.3 Hyperparameters:

The following hyperparameters are used mentioned below:

Binary Class Segmentation: Image size = 320x320, Batch size = 8, dice & focal loss, Adam optimizer with learning rate = 0.0001, 20 epochs in total with early stopping.

Multi-class Segmentation: Image size = 256x256 (Zenodo) and 512x512 (Medical Segmentation), Batch size = 16, total loss which is a combination of weighted binary cross entropy, focal loss and twesvky loss, Adam optimizer with learning rate = 0.0001, 25 epochs in total with early stopping.

5.3.4 Evaluation Metrics:

For the Segmentation problem, Jaccard Index & F1-score are used for evaluation.

$$\text{Jaccard index} = \frac{TP}{TP + FP + FN} \quad (5.3.1)$$

$$\text{F1Score} = \frac{2TP}{2TP + FP + FN} \quad (5.3.2)$$

CHAPTER 6

Experimental Results

6.1 Results

The results of classification and segmentation proposed architectures will be discussed in this section.

6.1.1 Performance of the Binary Class Classification:

The binary classifier was implemented on three datasets and consists of two datasets for CT scans & one for X-ray scans namely "*SARS COV II, IEEE-8023, COVID CT DS GitHub*". Accuracy, precision, recall and F1-score were the measurement methods employed. All of the results have been summarized in Table 6.2.

Train Test Split: The *COVID CT* dataset includes 349 COVID CT scans and 195 healthy CT scans, with 408 utilised for training and 136 for testing. Similarly, the *SARS COV II* Dataset includes 1252 COVID images as well as 1229 non-COVID images. 1860 images were utilised for training and 621 images were used for testing, using a train test split of 20%. Finally, the *IEEE 8023* X-ray dataset includes 940 X-ray images, 435 of which are positive COVID X-rays and 505 of which are healthy X-rays. Using a 20% train-test split, 752 x-rays were utilised for training and 188 for testing. Table 6.1 shows the ratio of the train test split.

Results: For binary class classification, we compared 9 deep learning architectures result with other state of the art architectures and methods on three COVID-19's binary

Table 6.1: Train Test Split for Binary Class Classification

Dataset	Total Number of Images	Training	Testing
SARS COV II	2481	1860	621
COVID CT DS GitHub	544	408	136
IEEE-8023	940	752	188

class datasets and the performance of the model was compared using the accuracy's, precision, recall and F1-Score of the test dataset. A closer inspection of the table 6.2 reveals that DL architectures are reliable for diagnosing COVID-19. Resnet 101 V2 architecture emerges the best with maximal accuracy of 96% and 97% on "*COVID CT DS GitHub & IEEE-8023 X-ray dataset*" while VGG-16 architecture performs best with a maximal accuracy of 98% on *SARS COV II CT dataset*.

The confusion matrices for the binary classification results of all three dataset are shown in Fig 6.1, 6.2, 6.3.

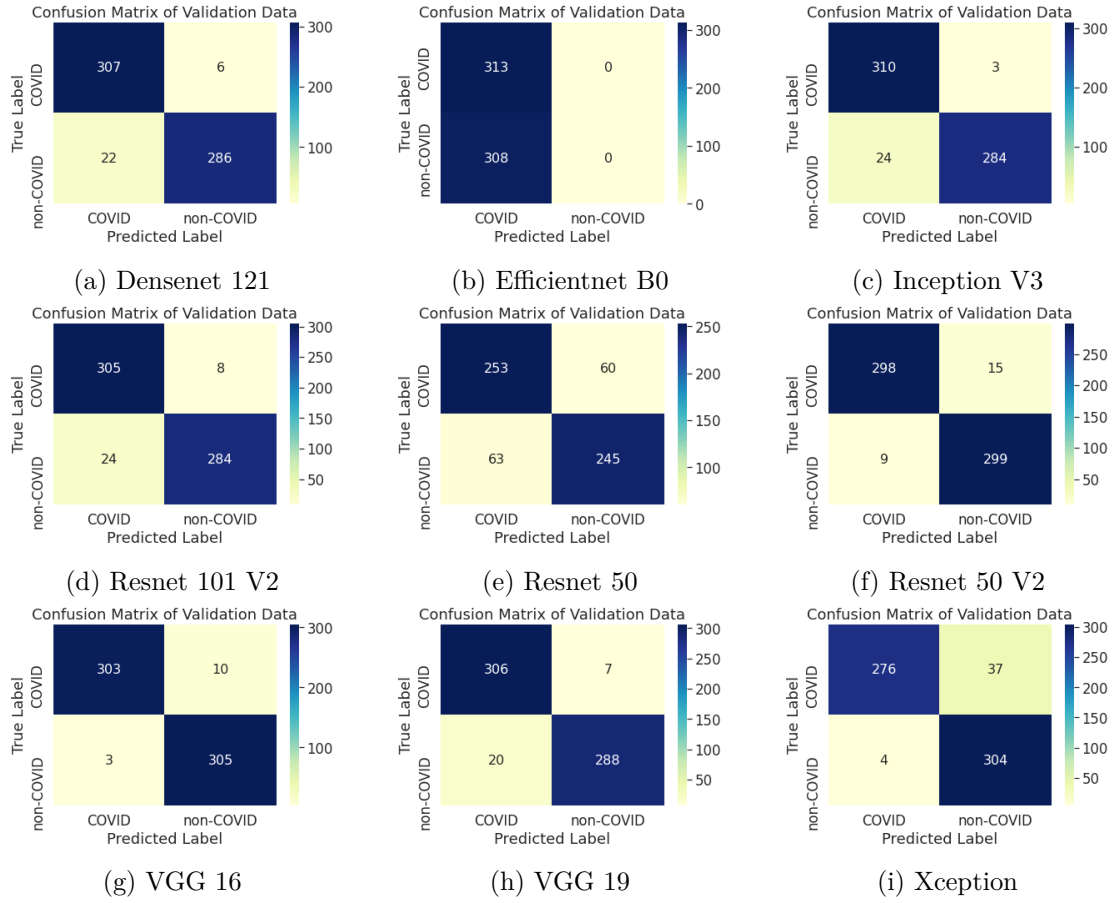


Figure 6.1: Confusion Matrix of SARS COV II CT Dataset

CHAPTER 6: EXPERIMENTAL RESULTS

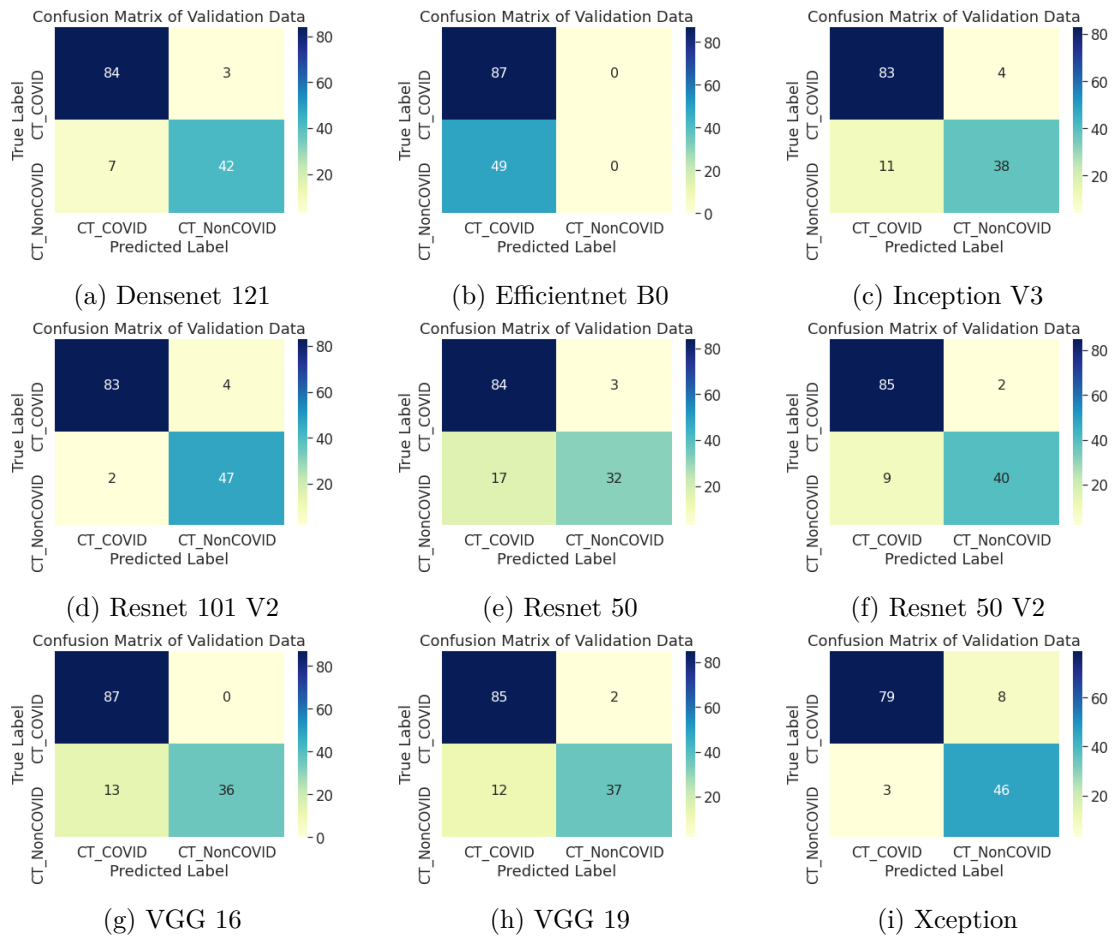


Figure 6.2: Confusion Matrix of COVID-CT Dataset

CHAPTER 6: EXPERIMENTAL RESULTS

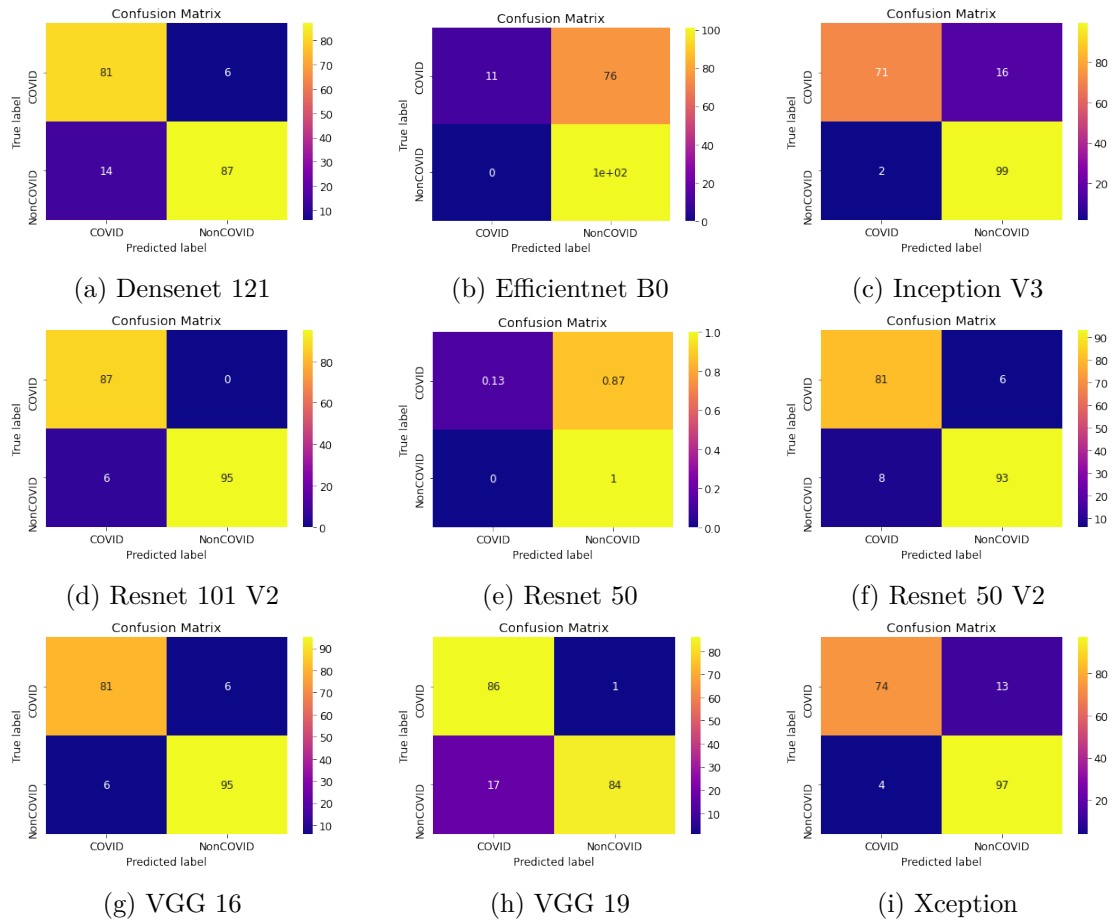


Figure 6.3: Confusion Matrix of IEEE 8023 Dataset

Table 6.2: Evaluation Metrics for Binary Classification

Datasets	Model	Accuracy	Precision	Recall	F1-Score
<i>IEEE 8023 X-ray (Binary class) [24]</i>	VGG-16	0.94	0.94	0.94	0.94
	VGG-19	0.90	0.91	0.91	0.90
	Xception	0.91	0.92	0.91	0.91
	ResNet 50 V2	0.93	0.92	0.93	0.93
	Inception V3	0.90	0.92	0.90	0.90
	Res Net 101 V2	0.97	0.97	0.97	0.97
	Dense Net 121	0.89	0.89	0.90	0.89
	ResNet 50	0.60	0.79	0.56	0.48
	Efficient net B0	0.60	0.79	0.58	0.49
	Xception	0.93	0.88	0.99	0.93
<i>SARS COV II CT Scan DS (Binary class) [20]</i>	Inception V3	0.96	0.99	0.93	0.96
	Dense Net 121	0.95	0.98	0.93	0.96
	VGG-16	0.98	0.97	0.99	0.98
	VGG-19	0.96	0.98	0.94	0.96
	ResNet-50	0.80	0.81	0.80	0.80
	Resnet50v2	0.96	0.95	0.97	0.96
	Resnet101v2	0.95	0.97	0.93	0.95
	Efficientnet B0	0.50	1.00	0.50	0.67
	VGG-16	0.90	1.00	0.87	0.93
	VGG-19	0.90	0.98	0.88	0.92
<i>COVID CT DS GitHub (Binary class) [21]</i>	Xception	0.92	0.85	0.96	0.90
	ResNet 50 V2	0.92	0.98	0.90	0.94
	Inception V3	0.89	0.95	0.88	0.92
	Res Net 101 V2	0.96	0.95	0.98	0.97
	Dense Net 121	0.93	0.97	0.92	0.94
	Efficient Net B0	0.64	1.00	0.64	0.78
	ResNet 50	0.85	0.97	0.83	0.89
	VGG-16	0.90	1.00	0.87	0.93
	VGG-19	0.90	0.98	0.88	0.92
	Xception	0.92	0.85	0.96	0.90

6.1.2 Performance of the Multi-Class Classification:

The Multi class classification was implemented using COVID-19 radiography database with includes chest X-ray images of normal, viral pneumonia and the COVID-19 positive cases. The evaluation methods used were accuracy, precision, recall and F1-score. In Table 6.4, all findings are summarized.

Table 6.3: Train Test Split for Multi-Class Classification

Dataset	Total Number of Images	Training	Validation	Testing
Radiography Database (Kaggle)	15153 Normal = 10.2k COVID = 3616 Pneumonia = 1345	10606	3030	1517

Train Test Split: A total of 15153 images were used for this experiment in which 3616 images were positive COVID-19 images, 10.2k normal X-ray images and 1345 viral pneumonia. Using the Keras data image generator, the images were split into three groups. 10606 images were used for training, 3030 images for validation and 1517

images for testing. Table 6.3 show all the details.

Results: For Multi-class classification, we have utilized 12 deep learning architectures and compared it with other state of the art architectures. A closer examination of the table 6.4 shows that deep learning architectures are reliable even for multi class classification of the COVID-19 disease. In terms of greatest accuracy, the architecture of Resnet (50-V2) was indeed the best with an accuracy of 95%.

Table 6.4: Evaluation Metrics for Multi class Classification

Datasets	Model	Accuracy	Precision	Recall	F1-Score
10*COVID-19 Radiography Database [22, 23]	Xception	0.87	0.88	0.82	0.84
	Inception V3	0.85	0.89	0.70	0.75
	Nasnet Large	0.89	0.87	0.87	0.87
	ResNet-50 V2	0.95	0.93	0.88	0.90
	Dense Net 121	0.89	0.91	0.84	0.87
	Mobile Net V2	0.91	0.90	0.89	0.89
	VGG-16	0.80	0.83	0.67	0.69
	VGG-19	0.79	0.80	0.69	0.72
	Resnet 50	0.81	0.78	0.89	0.81
	Efficientnet B0	0.67	0.70	0.68	0.65
	Inception Resnet V2	0.90	0.91	0.80	0.84
	Resnet 101 V2	0.91	0.94	0.85	0.89

The confusion matrix, loss & accuracy plots for multi-class data set classification results are displayed in fig 6.4, 6.5 & 6.6 respectively:

Table 6.5: Overview of methods and quantitative results toward COVID-19 classification

Author	Dataset	Method	Results (Accuracy)
Alshazly [37]	SARS COV II	Xception / Densenet 121 / 169	0.88 / 0.87 / 0.85
Nguyen [39]	SARS COV II	Densenet 169 / Resnet 50	0.80 / 0.83
Hasan [40]	SARS COV II	CVR Net	0.78
Martinez [36]	SARS COV II	Densenet 169 / 121	0.87 / 0.85
Proposed	SARS COV II	VGG-16	0.98
Panwar [75]	COVID CT DS GitHub	VGG-19	0.94
Wang [76]	COVID CT DS GitHub	COVID Net	0.90
Proposed	COVID CT DS GitHub	Resnet 101 V2	0.96
Horry [42]	IEEE 8023	VGG-16	0.79
Arellano [77]	IEEE 8023	Densenet 121	0.94
Militante [44]	IEEE 8023	VGG-16	0.95
Proposed	IEEE 8023	Resnet 101 V2	0.97
Proposed	Radiography DS	Resnet 50 V2	0.95
Maguolo [78]	Radiography DS	LOCO	0.79
Enxo [79]	Radiography DS	Resnet 18	0.85

CHAPTER 6: EXPERIMENTAL RESULTS

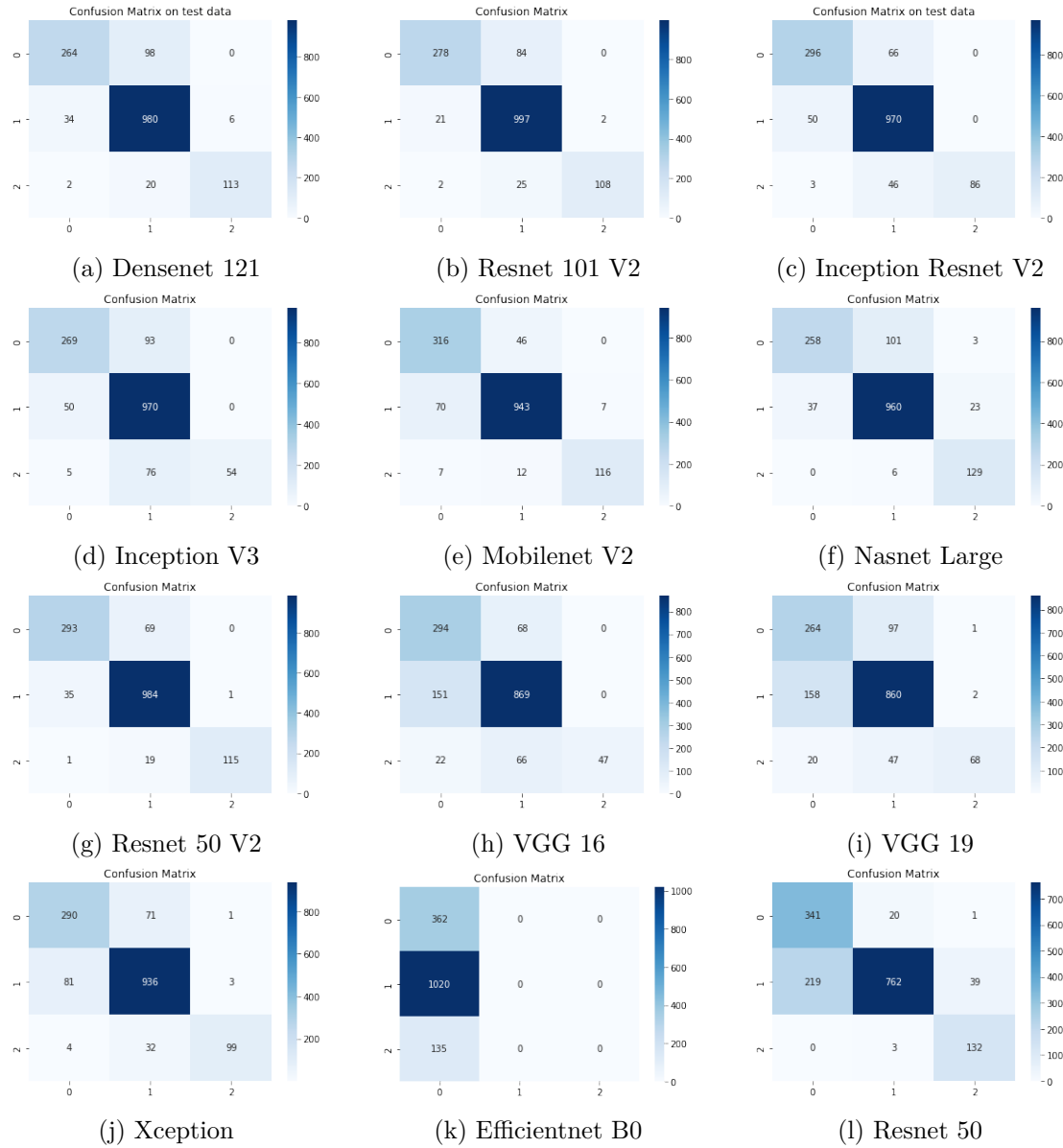


Figure 6.4: Confusion Matrix of X-ray Radiography Dataset

CHAPTER 6: EXPERIMENTAL RESULTS

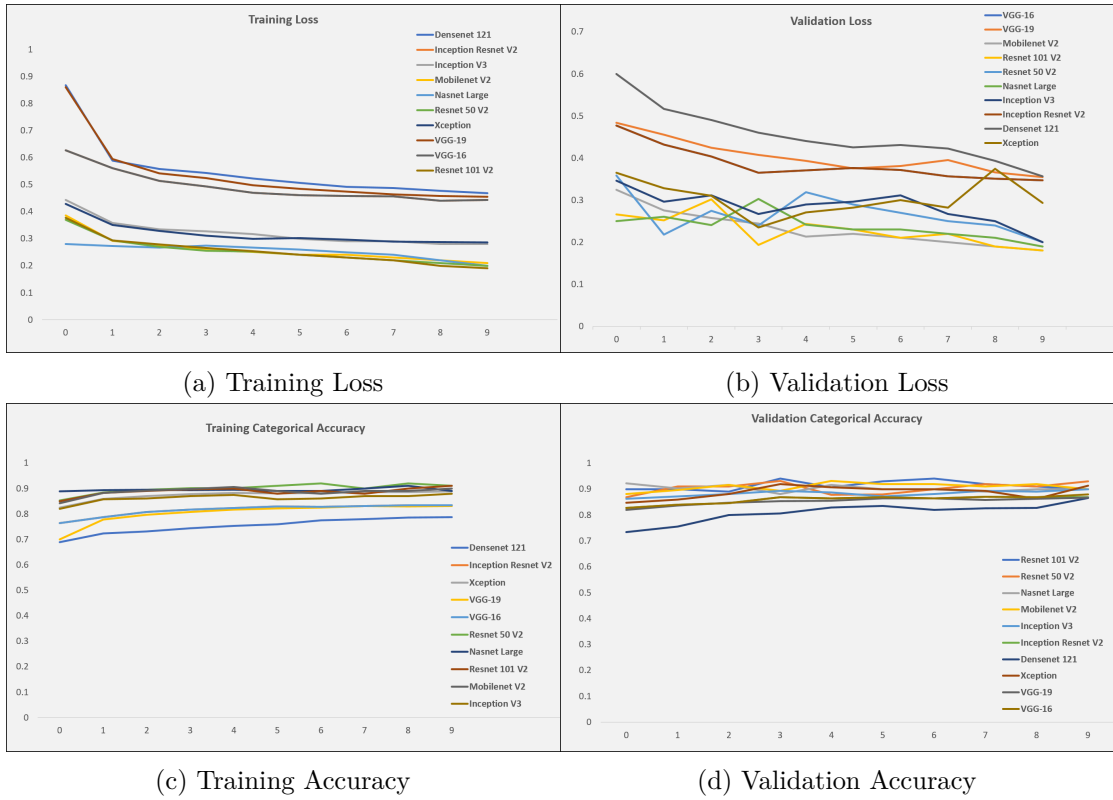


Figure 6.5: Loss & Accuracy of X-ray Radiography Dataset

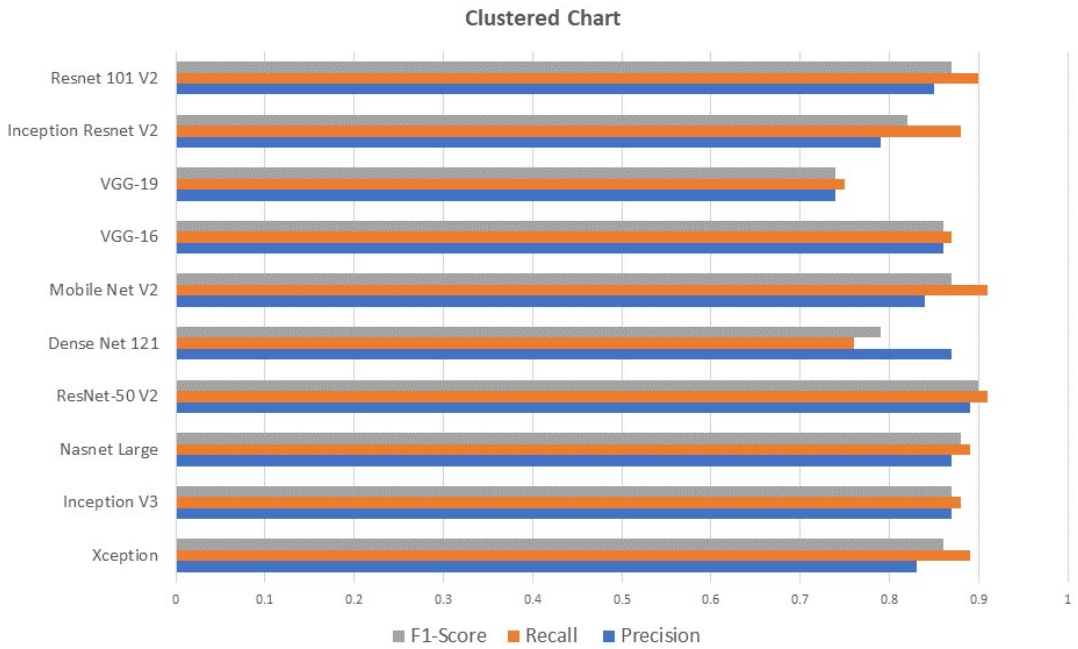


Figure 6.6: Precision, Recall & F1-Score of Multi-class Dataset

6.1.3 Performance of the Binary Class Segmentation:

The binary class segmentation was implemented on Zenodo dataset. Jaccard Index & F1-Score were the evaluation metrics employed. All the results have been summarized in Table 6.7.

Train Test Split: For binary class segmentation, two classes were segmented: "background and disease." Using the synthetic image creation theme for data augmentation, a total of 1000 CT images were used for this experiment. 500 images for training, 300 for validation and 200 for testing. Table 6.6 show details for the train, test, split.

Table 6.6: Train Test Split for Binary Class Segmentation

Original Number of Images	After Data Augmentation	Training	Validation	Testing
20	1000	500	300	200

Results: A close examination of the table 6.7 reveals that all of the architectures with respected backbones showed the maximum Jaccard Index and F1-Score, although the Unet architecture with Mobilenet V2 as encoder (backbone) performed somewhat better attaining an overall F1-Score of 98% on test dataset. The mean F1-Score for each architecture is 97.33% for Unet, 95.33% for PSPNet, 96.83% for Linknet and 92.83% for FPN.

Deep learning architectures are dependable for semantic segmentation of COVID-19 images. The architecture of Unet is indeed the finest one in terms of the highest F1 score.

6.1.4 Performance of the Multi Class Segmentation:

The multi class segmentation was carried out on the Zenodo dataset and Medical Segmentation dataset utilizing the background masks, lungs masks and diseases masks for segmentation on the Zenodo Data and the ground glass, consolidation, lungs and background masks for medical segmentation. Details for the train, test, split is mentioned in table 6.8. The assessment metrics used for the evaluation were Jaccard Index and the F1-Score. Table 6.11 summarizes all the results.

Table 6.7: Evaluation Metrics for Binary Segmentation

Dataset	Mode	Architecture	Backbone	Jaccard Index	F1-Score
Zenodo	Binary class	Unet	Efficient Net B3	0.943	0.970
			Mobile Net V2	0.972	0.986
			Inception Resnet V2	0.970	0.985
			Dense Net 121	0.943	0.970
			SeresNet 101	0.927	0.962
			VGG19	0.915	0.955
		PSPNet	Efficient Net B3	0.927	0.962
			Mobile Net V2	0.932	0.964
			Inception Resnet V2	0.956	0.977
			Dense Net 121	0.957	0.977
			SeresNet 101	0.915	0.955
			VGG19	0.854	0.921
		Linknet	Efficient Net B3	0.921	0.958
			Mobile Net V2	0.961	0.980
			Inception Resnet V2	0.961	0.980
			Dense Net 121	0.915	0.955
			SeresNet 101	0.949	0.973
			VGG19	0.957	0.977
		FPN	Efficient Net B3	0.921	0.958
			Mobile Net V2	0.940	0.969
			Inception Resnet V2	0.959	0.979
			Dense Net 121	0.928	0.962
			SeresNet 101	0.965	0.982
			VGG19	0.886	0.939

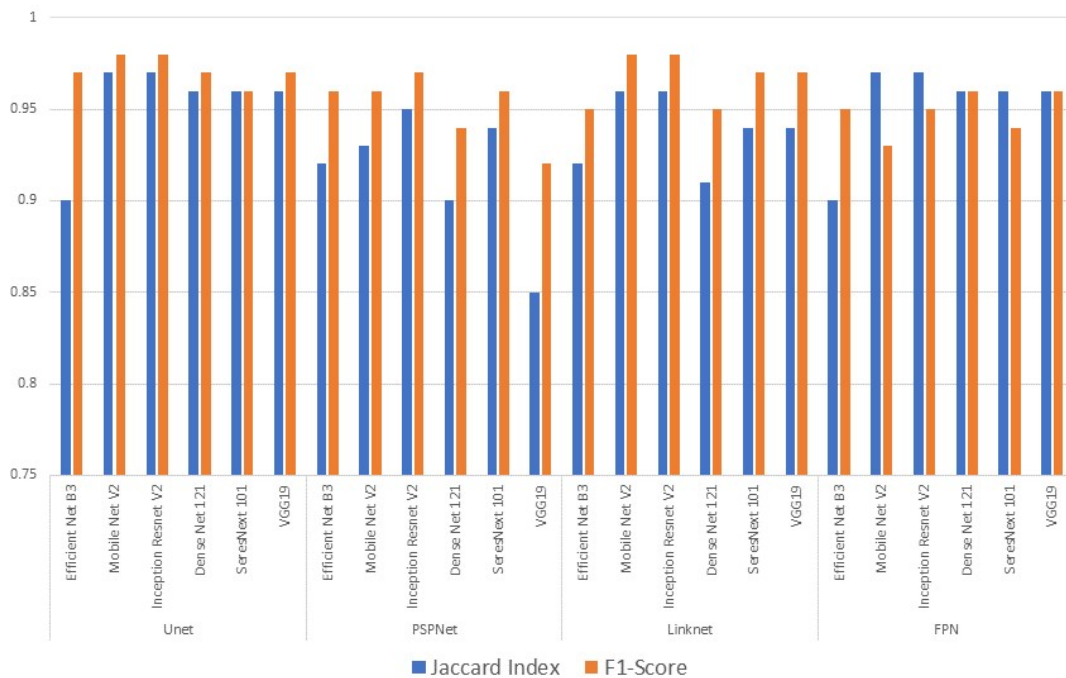


Figure 6.7: Jaccard Index & F1-Score of Binary Class Segmentation

CHAPTER 6: EXPERIMENTAL RESULTS

All the available backbones with all architectures were tested and time was taken about one day with one backbone on one architecture on Google Colab

Train Test Split: On the first experiment using the medical segmentation dataset, four classes were segmented: ‘ground glass, consolidation, lungs and background” using the medical segmentation dataset. Ground glass opacity (GGO) refers to the hazy grey regions that may be seen in lungs CT scans or X-rays. The grey patches represent increased density throughout the lungs. Lung consolidation is when the air that normally fills the tiny airways in the lungs gets replaced with something else like fluid such as pus, blood, or water, a solid such as stomach contents or cells. The medical segmentation dataset has two subset dataset "Radiopedia and Medseg". For the radiopedia part, out of 829 slices of images, 580 images were used for training, 124 for validation and 125 for testing. For the Medseg part, 71 images were used for training, 14 for validation and 15 for testing. In total, 651 images were used for training, 138 for validation and 140 for testing. On the second experiment using the zenodo dataset, four classes were segmented “background, right lung, left lung, disease”. Using the data image augmentation, 2840 Ct images were used for training, 680 for validation and 500 for testing.

Table 6.8: Train Test Split for Multi-Class Segmentation

Dataset	Original Number of Images	Augmentation	Training	Validation	Testing
Medical Segmentation	829+100	No	580+71	124+14	125+15
Zenodo	20	Yes	2840	680	500

Results: For the medical Segmentation dataset, a detailed analysis at the table 6.9 indicates that all of the architectures with respected backbones had the best F1-Score for multi-class segmentation, while the Linknet architecture with Inception Resnet V2 as encoder performed better with an overall Jaccard Index of 68% and F1-Score of 75% on the test dataset. Each architecture has a mean F1-Score of 72.16% for Linknet, 70.50% for Unet and FPN, and 69.00% for PSPNet. As Linknet is a light deep neural network architecture, it performed well in semantic segmentation, with the capacity to provide real-time performance on both GPUs and embedded devices such as the NVIDIA TX1. Similarly for the Zenodo Dataset, a deeper examination at the table 6.9 shows that all DL architectures with respected backbones had the best F1-Score, while the FPN

CHAPTER 6: EXPERIMENTAL RESULTS

architecture with Densenet 121 as encoder excelled at extracting masks for image segmentation on this dataset, with an overall Jaccard Index of 70% F1-Score of 77% on the test dataset. FPN has achieved a mean F1-Score of 73.33%, Unet has a score of 72.66%, Linknet has a score of 69.50%, and PSPNet has a score of 66.33%.

The visual aspect of segmented images of both data sets is illustrated by Fig 6.14 & 6.15. The yellow region is the true positive i.e "an outcome where the model correctly predicts the positive class" Red region is false positive i.e "an outcome where the model incorrectly predicts the positive class" & green region is false negative i.e " an outcome where the model incorrectly predicts the negative class".

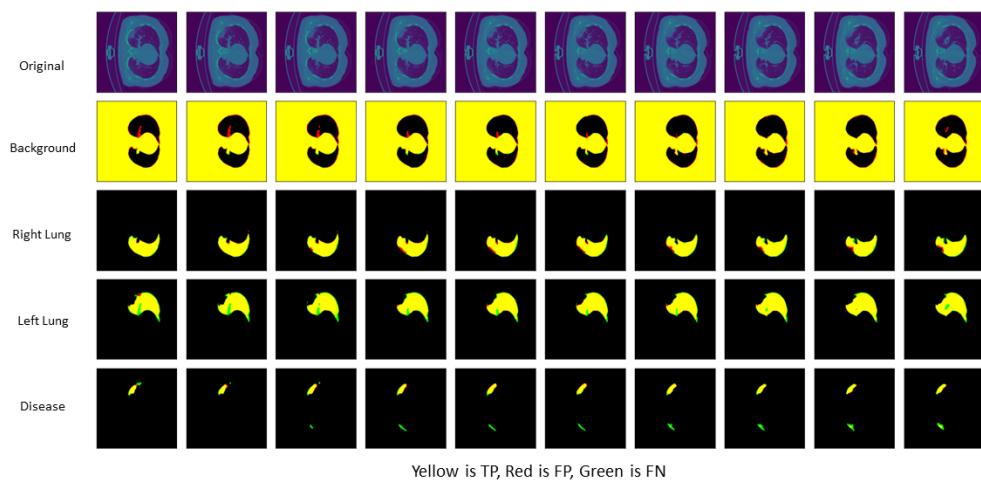


Figure 6.8: Visual Appearance of COVID-19 Segmented Images of Zenodo Dataset

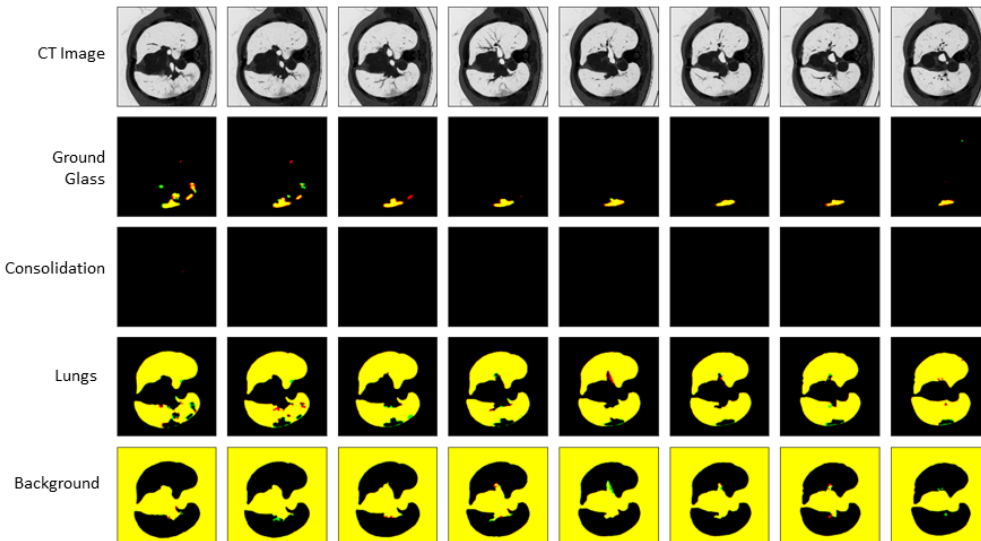


Figure 6.9: Visual Appearance of COVID-19 Segmented Images of Medical Segmentation Dataset

CHAPTER 6: EXPERIMENTAL RESULTS

Table 6.9: Evaluation Metrics for Multi class Segmentation

Dataset	Mode	Architecture	Backbone	Jaccard Index	F1-Score
Zenodo	Multi class	Unet	Efficient Net B3	0.66	0.72
			Mobile Net V2	0.65	0.72
			Inception Resnet V2	0.67	0.73
			Dense Net 121	0.68	0.74
			SeresNet 101	0.69	0.75
			VGG19	0.64	0.70
		PSPNet	Efficient Net B3	0.53	0.60
			Mobile Net V2	0.48	0.54
			Inception Resnet V2	0.64	0.71
			Dense Net 121	0.66	0.72
			SeresNet 101	0.59	0.67
			VGG19	0.67	0.74
		Linknet	Efficient Net B3	0.68	0.74
			Mobile Net V2	0.65	0.71
			Inception Resnet V2	0.69	0.76
			Dense Net 121	0.56	0.63
			SeresNet 101	0.63	0.69
			VGG19	0.58	0.64
		FPN	Efficient Net B3	0.64	0.70
			Mobile Net V2	0.62	0.69
			Inception Resnet V2	0.69	0.76
			Dense Net 121	0.70	0.77
			SeresNet 101	0.68	0.74
			VGG19	0.68	0.74
Medical Segmentation	Multi class	Unet	Efficient Net B3	0.64	0.72
			Mobile Net V2	0.63	0.69
			Inception Resnet V2	0.66	0.74
			Dense Net 121	0.60	0.68
			SeresNet 101	0.65	0.73
			VGG19	0.60	0.67
		PSPNet	Efficient Net B3	0.62	0.69
			Mobile Net V2	0.53	0.61
			Inception Resnet V2	0.64	0.72
			Dense Net 121	0.66	0.73
			SeresNet 101	0.66	0.74
			VGG19	0.56	0.64
		Linknet	Efficient Net B3	0.66	0.74
			Mobile Net V2	0.65	0.74
			Inception Resnet V2	0.68	0.75
			Dense Net 121	0.60	0.68
			SeresNet 101	0.66	0.73
			VGG19	0.61	0.68
		FPN	Efficient Net B3	0.65	0.72
			Mobile Net V2	0.60	0.67
			Inception Resnet V2	0.65	0.72
			Dense Net 121	0.66	0.74
			SeresNet 101	0.65	0.73
			VGG19	0.58	0.65

CHAPTER 6: EXPERIMENTAL RESULTS

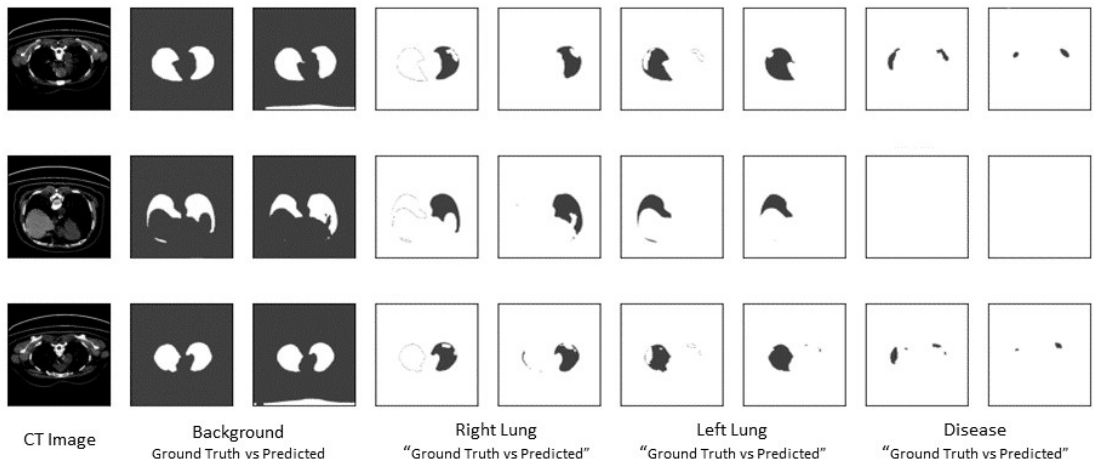


Figure 6.10: Ground Truth vs Predicted of COVID-19 Segmentation

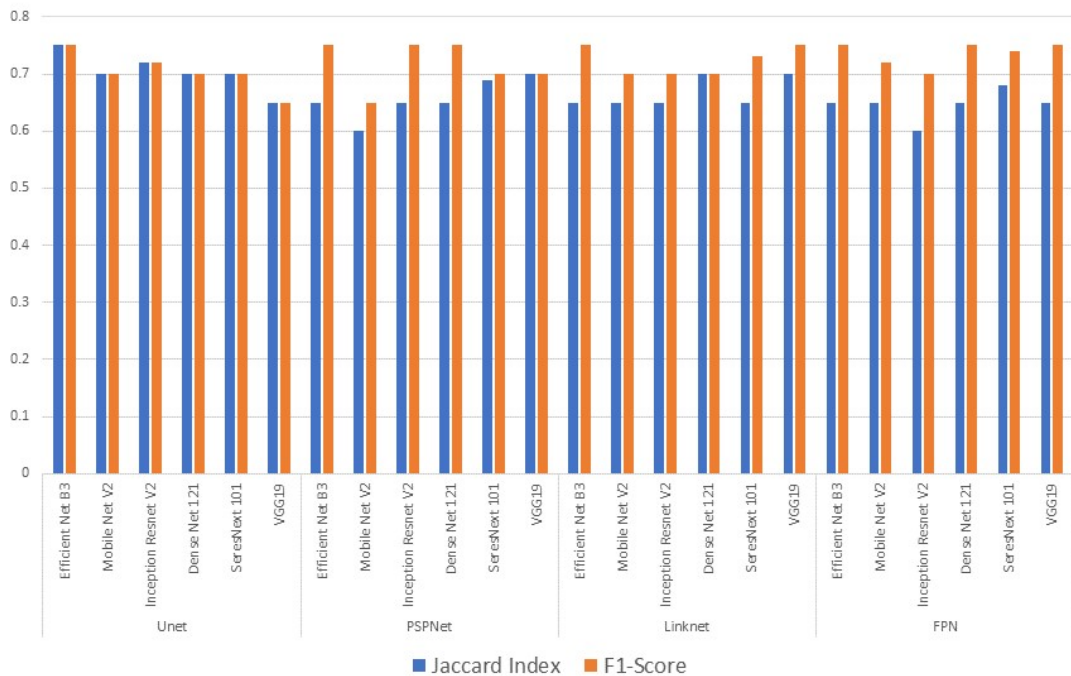


Figure 6.11: Jaccard Index & F1-Score of Multi Class Zenodo Dataset

CHAPTER 6: EXPERIMENTAL RESULTS

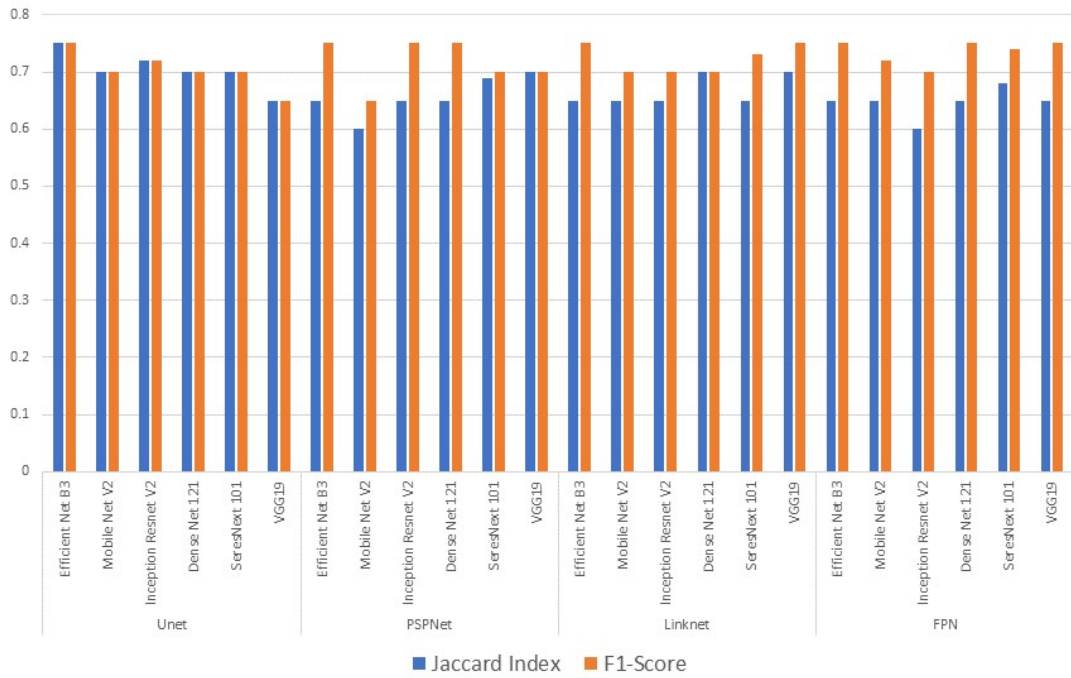


Figure 6.12: Jaccard Index & F1-Score of Multi Class Medical Segmentation Dataset

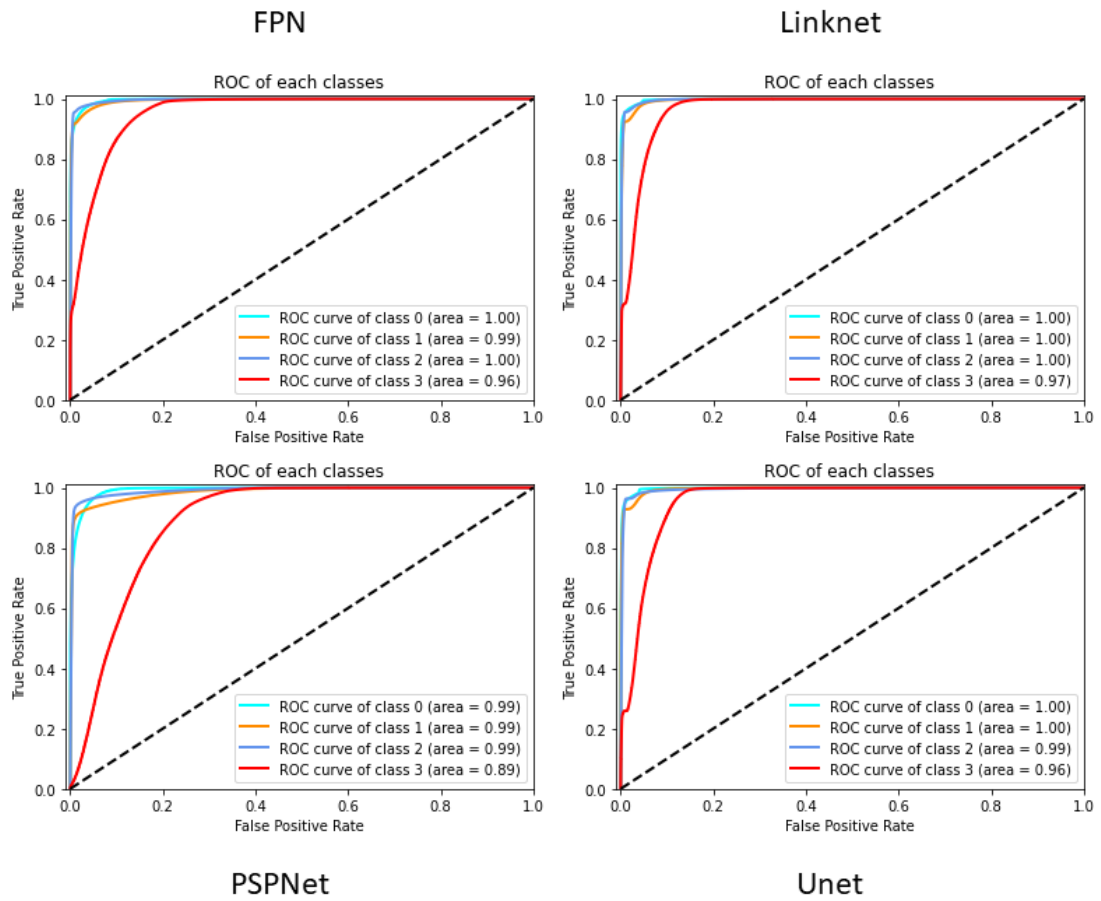


Figure 6.13: ROC Curves

Table 6.10: Comparison of proposed model to various state of the art baseline classification and segmentation approaches

Mode	Dataset	Author	Method	Results
Classification	SARS COV II	H.Alshazly[37]	Xception / Densenet 121-169	0.88 / 0.87 / 0.85
		Nguyen[39]	Densenet 169 / Resnet 50	0.80 / 0.83
		Hassan[40]	CVR Net	0.78
		Martinez[36]	Densenet 169-121	0.87 / 0.75
		Proposed	VGG-16	0.98
	COVID CT DS	Panwar[75]	VGG-19	0.94
		Wang[46]	COVID Net	0.90
		Mine Amyar[80]	Multi task DL approach	0.94
		Proposed	Resnet 101 V2	0.96
	IEEE-8023	Horry[42]	VGG-16	0.79
		Arellano[77]	Densenet 121	0.94
		Militante[44]	VGG-16	0.95
		Proposed	Resnet 101 V2	0.97
Segmentation	Radiography Database	Maguolo[78]	LOCO	0.79
		Enxo[79]	Resnet 18	0.85
		Proposed	Resnet 50 V2	0.95
		Deng Ping Fan[81]	Inf Net	0.68
		Olaf Ronneberger	Unet	0.70
	Medical Segmentation	Vijay[48]	Segnet	0.50
		Yixin Wang[82]	Hybrid Encoder	0.70
		Proposed	FPN. Densenet 121	0.77
	Zenodo (Binary Class)	Adnan Saood[48]	Unet	0.55
		Proposed	Linknet. Inception Resnet V2	0.75
	Zenodo (Multi Class)	Dominik[49]	3D Unet	0.76
		Proposed	Unet. Mobile net V2	0.98

CHAPTER 7

Conclusion

With COVID-19 now a worldwide danger & killing hundreds of thousands of lives, we provided a detailed comparison of several deep learning architectures for image classification and image segmentation in this research. We suggested various alternative deep learning architectures for image classification and image segmentation to solve the shortage of minimalistic training material and fulfill the efficiency requirement of CAD deployment. In addition, we provide a thorough benchmark that will be beneficial for future studies.

We trained several deep learning models for classification. The first one is a binary classification that aims to separate CT and X-ray images of COVID-19 and non-COVID-19 cases. Then we performed multi-class classification that aims to separate X-ray images of COVID-19, normal and viral pneumonia cases. It reaches a maximum accuracy of 98% for binary class & 95% for multi class classification.

Moreover, we also performed and trained several deep learning models for the binary and multi-class image segmentation. The results shows that deep learning architectures are reliable for COVID-19 image segmentation. Unet architecture are the greatest in the top F1 scoring of 98% for binary class segmentation and 77% for multi-class segmentation.

The results demonstrate that not only do these deep learning architectures aid in the classification of COVID-19 CT and X-ray images, but they can also determine the specific site of the COVID-19 infection. These architectures can help in CAD systems and can assist radiologists to correctly and fastly detect the COVID-19 using radiological imaging in less time.

7.1 Future Work

As the future work, we can propose:

- Experimenting the proposed framework with other COVID-19 datasets as it become available.
- Using traditional and non-AI techniques to evaluate the proposed framework.
- In the proposed segmentation architecture, investigating the effects of higher input resolution and different types of other encoders.
- Exploring the effect of higher input resolution for classification.

References

- [1] Lungs anatomy. URL <https://www.enchantedlearning.com/subjects/anatomy/lungs/>.
- [2] Nicole Jawerth. A window inside the body and covid-19, year = 2020, url = <https://www.iaea.org/bulletin/infectious-diseases/a-window-inside-the-body-and-covid-19>.
- [3] Levity. URL <https://levity.ai/>.
- [4] Machine learning and deep learning 101 - networking technologies. <https://www.net-cloud.com/blog/machine-learning-and-deep-learning-101/>.
- [5] Dog breed identification with fine tuning of pre-trained models. <https://www.ijrte.org/wp-content/uploads/papers/v8i2S11/B14640982S1119.pdf>.
- [6] Convolution neural network for image processing — using keras | by angel das | towards data science. <https://towardsdatascience.com/convolution-neural-network-for-image-processing-using-keras-dc3429056306>, .
- [7] Neural convolutional layers. <https://m-alcu.github.io/blog/2018/01/13/neural-layers/>.
- [8] 9.5 neural networks | analysis of 2019 kaggle ml & ds survey. <http://machinelearningintro.uwesterr.de/MLAlgoNN.html>.
- [9] Understand the architecture of cnn | by kousai smeda | towards data science. <https://towardsdatascience.com/understand-the-architecture-of-cnn-90a25e244c7>.
- [10] Devi Frossard. Vgg in tensorflow. URL <https://www.cs.toronto.edu/~frossard/post/vgg16/>.

REFERENCES

- [11] Gao Huang, Zhuang Liu, Laurens Van Der Maaten, and Kilian Q Weinberger. Densely connected convolutional networks. In *Proceedings of the IEEE conference on computer vision and pattern recognition*, pages 4700–4708, 2017.
- [12] Resnet (34, 50, 101): Residual cnns for image classification tasks. <https://neurohive.io/en/popular-networks/resnet/>.
- [13] Review: Mobilenetv2 — light weight model (image classification) | by sik-ho tsang | towards data science. <https://towardsdatascience.com/review-mobilenetv2-light-weight-model-image-classification-8febb490e61c>,
- .
- [14] Xception: Implementing from scratch using tensorflow | by arjun sarkar | towards data science. <https://towardsdatascience.com/xception-from-scratch-using-tensorflow-even-better-than-inception-940fb231ced9>.
- [15] Inception-resnet-v2-b explained | papers with code. <https://paperswithcode.com/method/inception-resnet-v2-b>.
- [16] The network architecture of efficientnet. it can output a feature map... | download scientific diagram. https://www.researchgate.net/figure/The-network-architecture-of-EfficientNet-It-can-output-a-feature-map-with-deep-sfig3_349299852.
- [17] Review: Nasnet — neural architecture search network (image classification) | by sik-ho tsang | medium. <https://sh-tsang.medium.com/review-nasnet-neural-architecture-search-network-image-classification-23139ea0428>,
- .
- [18] qubvel/segmentation_models: Segmentation models with pretrained backbones. keras and tensorflow keras. https://github.com/qubvel/segmentation_models.
- [19] Review of deep learning: concepts, cnn architectures, challenges, applications, future directions | journal of big data | full text. <https://journalofbigdata.springeropen.com/articles/10.1186/s40537-021-00444-8>.
- [20] Plamen Angelov and Eduardo Almeida Soares. Sars-cov-2 ct-scan dataset: A large dataset of real patients ct scans for sars-cov-2 identification. *MedRxiv*, 2020.

REFERENCES

- [21] Xingyi Yang, Xuehai He, Jinyu Zhao, Yichen Zhang, Shanghang Zhang, and Pengtao Xie. Covid-ct-dataset: a ct scan dataset about covid-19. *arXiv preprint arXiv:2003.13865*, 2020.
- [22] Muhammad EH Chowdhury, Tawsifur Rahman, Amith Khandakar, Rashid Mazhar, Muhammad Abdul Kadir, Zaid Bin Mahbub, Khandakar Reajul Islam, Muhammad Salman Khan, Atif Iqbal, Nasser Al Emadi, et al. Can ai help in screening viral and covid-19 pneumonia? *IEEE Access*, 8:132665–132676, 2020.
- [23] Tawsifur Rahman, Amith Khandakar, Yazan Qiblawey, Anas Tahir, Serkan Kiranyaz, Saad Bin Abul Kashem, Mohammad Tariqul Islam, Somaya Al Maadeed, Susu M Zughraier, Muhammad Salman Khan, et al. Exploring the effect of image enhancement techniques on covid-19 detection using chest x-ray images. *Computers in biology and medicine*, 132:104319, 2021.
- [24] Joseph Paul Cohen, Paul Morrison, Lan Dao, Karsten Roth, Tim Q Duong, and Marzyeh Ghassemi. Covid-19 image data collection: Prospective predictions are the future. *arXiv preprint arXiv:2006.11988*, 2020.
- [25] Covid-19 ct segmentation dataset. 2020. URL <http://medicalsegmentation.com/covid19/>.
- [26] Covid-19 ct lung and infection segmentation dataset. 2020. URL <https://zenodo.org/record/3757476#.YWvaavpBzIU>.
- [27] Confusion matrix for your multi-class machine learning model | by joydwip mohajon | towards data science. <https://towardsdatascience.com/confusion-matrix-for-your-multi-class-machine-learning-model-ff9aa3bf7826>, .
- [28] Junaid Shuja, Eisa Alanazi, Waleed Alasmary, and Abdulaziz Alashaikh. Covid-19 open source data sets: A comprehensive survey. *Applied Intelligence*, pages 1–30, 2020.
- [29] MJ Keeling, TD Hollingsworth, and JM Read. The efficacy of contact tracing for the containment of the 2019 novel coronavirus (covid-19). medrxiv 2020. 02.14. 20023036. *Google Scholar*, 2020.
- [30] Chih-Cheng Lai, Yen Hung Liu, Cheng-Yi Wang, Ya-Hui Wang, Shun-Chung Hsueh, Muh-Yen Yen, Wen-Chien Ko, and Po-Ren Hsueh. Asymptomatic car-

REFERENCES

- rier state, acute respiratory disease, and pneumonia due to severe acute respiratory syndrome coronavirus 2 (sars-cov-2): Facts and myths. *Journal of Microbiology, Immunology and Infection*, 53(3):404–412, 2020.
- [31] Sebastian Hoehl, Holger Rabenau, Annemarie Berger, Marhild Kortenbusch, Jindrich Cinatl, Denisa Bojkova, Pia Behrens, Boris Böddinghaus, Udo Götsch, Frank Naujoks, et al. Evidence of sars-cov-2 infection in returning travelers from wuhan, china. *New England Journal of Medicine*, 382(13):1278–1280, 2020.
- [32] Tuan D Pham. A comprehensive study on classification of covid-19 on computed tomography with pretrained convolutional neural networks. *Scientific Reports*, 10(1):1–8, 2020.
- [33] Tulin Ozturk, Muhammed Talo, EYLUL AZRA YILDIRIM, Ulas Baran Baloglu, Ozal Yildirim, and U Rajendra Acharya. Automated detection of covid-19 cases using deep neural networks with x-ray images. *Computers in biology and medicine*, 121:103792, 2020.
- [34] Asif Iqbal Khan, Junaid Latief Shah, and Mohammad Mudasir Bhat. Coronet: A deep neural network for detection and diagnosis of covid-19 from chest x-ray images. *Computer Methods and Programs in Biomedicine*, 196:105581, 2020.
- [35] Tanvir Mahmud, Md Awsafur Rahman, and Shaikh Anowarul Fattah. Covxnet: A multi-dilation convolutional neural network for automatic covid-19 and other pneumonia detection from chest x-ray images with transferable multi-receptive feature optimization. *Computers in biology and medicine*, 122:103869, 2020.
- [36] Alejandro R Martinez. Classification of covid-19 in ct scans using multi-source transfer learning. *arXiv preprint arXiv:2009.10474*, 2020.
- [37] Hammam Alshazly, Christoph Linse, Erhardt Barth, and Thomas Martinetz. Explainable covid-19 detection using chest ct scans and deep learning. *Sensors*, 21(2):455, 2021.
- [38] Bin Liu, Xiaoxue Gao, Mengshuang He, Lin Liu, and Guosheng Yin. A fast online covid-19 diagnostic system with chest ct scans. In *Proceedings of KDD*, volume 2020, 2020.

REFERENCES

- [39] DMH Nguyen, DM Nguyen, H Vu, BT Nguyen, F Nunnari, and D Sonntag. An attention mechanism with multiple knowledge sources for covid-19 detection from ct images. 2020.
- [40] Md Hasan, Md Alam, Md Elahi, E Toufick, Shidhartho Roy, Sifat Redwan Wahid, et al. Cvr-net: A deep convolutional neural network for coronavirus recognition from chest radiography images. *arXiv preprint arXiv:2007.11993*, 2020.
- [41] Xiang Yu, Shui-Hua Wang, and Yu-Dong Zhang. Cgnet: A graph-knowledge embedded convolutional neural network for detection of pneumonia. *Information Processing & Management*, 58(1):102411, 2021.
- [42] Michael J Horry, Subrata Chakraborty, Manoranjan Paul, Anwaar Ulhaq, Biswajeet Pradhan, Manas Saha, and Nagesh Shukla. Covid-19 detection through transfer learning using multimodal imaging data. *IEEE Access*, 8:149808–149824, 2020.
- [43] Siti Raihanah Abdani, Mohd Asyraf Zulkifley, and Nuraisyah Hani Zulkifley. A lightweight deep learning model for covid-19 detection. In *2020 IEEE Symposium on Industrial Electronics & Applications (ISIEA)*, pages 1–5. IEEE, 2020.
- [44] Sammy V Militante, Nanette V Dionisio, and Brandon G Sibbaluca. Pneumonia and covid-19 detection using convolutional neural networks. In *2020 Third International Conference on Vocational Education and Electrical Engineering (ICVEE)*, pages 1–6. IEEE, 2020.
- [45] Prabira Kumar Sethy, Santi Kumari Behera, Pradyumna Kumar Ratha, and Preesat Biswas. Detection of coronavirus disease (covid-19) based on deep features and support vector machine. 2020.
- [46] Linda Wang, Zhong Qiu Lin, and Alexander Wong. Covid-net: A tailored deep convolutional neural network design for detection of covid-19 cases from chest x-ray images. *Scientific Reports*, 10(1):1–12, 2020.
- [47] Narges Saeedizadeh, Shervin Minaee, Rahele Kafieh, Shakib Yazdani, and Milan Sonka. Covid tv-unet: Segmenting covid-19 chest ct images using connectivity imposed unet. *Computer Methods and Programs in Biomedicine Update*, page 100007, 2021.

REFERENCES

- [48] Adnan Saood and Iyad Hatem. Covid-19 lung ct image segmentation using deep learning methods: U-net versus segnet. *BMC Medical Imaging*, 21(1):1–10, 2021.
- [49] Dominik Müller, Iñaki Soto Rey, and Frank Kramer. Automated chest ct image segmentation of covid-19 lung infection based on 3d u-net. *arXiv preprint arXiv:2007.04774*, 2020.
- [50] Amine Amyar, Romain Modzelewski, Hua Li, and Su Ruan. Multi-task deep learning based ct imaging analysis for covid-19 pneumonia: Classification and segmentation. *Computers in Biology and Medicine*, 126:104037, 2020.
- [51] Athanasios Voulodimos, Eftychios Protopapadakis, Iason Katsamenis, Anastasios Doulamis, and Nikolaos Doulamis. Deep learning models for covid-19 infected area segmentation in ct images. *medRxiv*, 2020.
- [52] Kai Gao, Jianpo Su, Zhongbiao Jiang, Ling-Li Zeng, Zhichao Feng, Hui Shen, Pengfei Rong, Xin Xu, Jian Qin, Yuexiang Yang, et al. Dual-branch combination network (dcn): Towards accurate diagnosis and lesion segmentation of covid-19 using ct images. *Medical image analysis*, 67:101836, 2021.
- [53] Yu Qiu, Yun Liu, Shijie Li, and Jing Xu. Miniseg: An extremely minimum network for efficient covid-19 segmentation, 2021.
- [54] Alex Noel Joseph Raj, Haipeng Zhu, Asiya Khan, Zhemin Zhuang, Zengbiao Yang, Vijayalakshmi GV Mahesh, and Ganesan Karthik. Adid-unet—a segmentation model for covid-19 infection from lung ct scans. *PeerJ Computer Science*, 7:e349, 2021.
- [55] Tongxue Zhou, Stéphane Canu, and Su Ruan. Automatic covid -19 ct segmentation using u-net integrated spatial and channel attention mechanism. *International Journal of Imaging Systems and Technology*, 31(1):16–27, Nov 2020. ISSN 1098-1098. doi: 10.1002/ima.22527. URL <http://dx.doi.org/10.1002/ima.22527>.
- [56] Omar Elharrouss, Nandhini Subramanian, and Somaya Al-Maadeed. An encoder-decoder-based method for covid-19 lung infection segmentation, 2020.
- [57] Yu-Huan Wu, Shang-Hua Gao, Jie Mei, Jun Xu, Deng-Ping Fan, Rong-Guo Zhang, and Ming-Ming Cheng. Jcs: An explainable covid-19 diagnosis system

REFERENCES

- by joint classification and segmentation. *IEEE Transactions on Image Processing*, 30:3113–3126, 2021. ISSN 1941-0042. doi: 10.1109/tip.2021.3058783. URL <http://dx.doi.org/10.1109/TIP.2021.3058783>.
- [58] Noreen Iftikhar. Breathtaking lungs: Their function and anatomy, 2018. URL <https://www.healthline.com/human-body-maps/lung>.
- [59] Neha Phatak. Coronavirus and covid-19: What you should know, 2021. URL <https://www.webmd.com/lung/coronavirus>.
- [60] Cleveland Clinic. Coronavirus, covid-19, 2020. URL <https://my.clevelandclinic.org/health/diseases/21214-coronavirus-covid-19>.
- [61] Yann LeCun, Yoshua Bengio, and Geoffrey Hinton. Deep learning. *nature*, 521(7553):436–444, 2015.
- [62] Ziwei Zhang, Peng Cui, and Wenwu Zhu. Deep learning on graphs: A survey. *IEEE Transactions on Knowledge and Data Engineering*, 2020.
- [63] Ajay Shrestha and Ausif Mahmood. Review of deep learning algorithms and architectures. *IEEE Access*, 7:53040–53065, 2019.
- [64] Maryam M Najafabadi, Flavio Villanustre, Taghi M Khoshgoftaar, Naeem Seliya, Randall Wald, and Edin Muharemagic. Deep learning applications and challenges in big data analytics. *Journal of big data*, 2(1):1–21, 2015.
- [65] Ian Goodfellow, Yoshua Bengio, and Aaron Courville. *Deep learning*. MIT press, 2016.
- [66] Connor Shorten, Taghi M Khoshgoftaar, and Borko Furht. Deep learning applications for covid-19. *Journal of big Data*, 8(1):1–54, 2021.
- [67] Luca Brunese, Francesco Mercaldo, Alfonso Reginelli, and Antonella Santone. Explainable deep learning for pulmonary disease and coronavirus covid-19 detection from x-rays. *Computer Methods and Programs in Biomedicine*, 196:105608, 2020.
- [68] Mohammad Jamshidi, Ali Lalbakhsh, Jakub Talla, Zdeněk Peroutka, Farimah Hadjilooei, Pedram Lalbakhsh, Morteza Jamshidi, Luigi La Spada, Mirhamed Mirmozafari, Mojgan Dehghani, et al. Artificial intelligence and covid-19: deep learning approaches for diagnosis and treatment. *Ieee Access*, 8:109581–109595, 2020.

REFERENCES

- [69] Mohammad Shorfuzzaman and M Shamim Hossain. Metacovid: A siamese neural network framework with contrastive loss for n-shot diagnosis of covid-19 patients. *Pattern recognition*, 113:107700, 2021.
- [70] Alex Krizhevsky, Ilya Sutskever, and Geoffrey E Hinton. Imagenet classification with deep convolutional neural networks. *Advances in neural information processing systems*, 25:1097–1105, 2012.
- [71] Karen Simonyan and Andrew Zisserman. Very deep convolutional networks for large-scale image recognition. *arXiv preprint arXiv:1409.1556*, 2014.
- [72] Kaiming He, Xiangyu Zhang, Shaoqing Ren, and Jian Sun. Deep residual learning for image recognition. *corr abs/1512.03385* (2015), 2015.
- [73] François Chollet. Xception: deep learning with depthwise separable convolutions. *corr abs/1610.02357* (2016). *arXiv preprint arXiv:1610.02357*, 2016.
- [74] Christian Szegedy, Sergey Ioffe, Vincent Vanhoucke, and Alex Alemi. Inception-v4, inception-resnet and the impact of residual connections on learning (2016). *arXiv preprint arXiv:1602.07261*, 2016.
- [75] Harsh Panwar, PK Gupta, Mohammad Khubeb Siddiqui, Ruben Morales-Menendez, Prakhar Bhardwaj, and Vaishnavi Singh. A deep learning and grad-cam based color visualization approach for fast detection of covid-19 cases using chest x-ray and ct-scan images. *Chaos, Solitons & Fractals*, 140:110190, 2020.
- [76] Zhao Wang, Quande Liu, and Qi Dou. Contrastive cross-site learning with re-designed net for covid-19 ct classification. *IEEE Journal of Biomedical and Health Informatics*, 24(10):2806–2813, 2020.
- [77] Matías Cam Arellano and Oscar E Ramos. Deep learning model to identify covid-19 cases from chest radiographs. In *2020 IEEE XXVII International Conference on Electronics, Electrical Engineering and Computing (INTERCON)*, pages 1–4. IEEE, 2020.
- [78] G Maguolo and L Nanni. A critic evaluation of methods for covid-19 automatic detection from x-ray images. arxiv 2020. *arXiv preprint arXiv:2004.12823*, 2020.

REFERENCES

- [79] Enzo Tartaglione, Carlo Alberto Barbano, Claudio Berzovini, Marco Calandri, and Marco Grangetto. Unveiling covid-19 from chest x-ray with deep learning: a hurdles race with small data. *International Journal of Environmental Research and Public Health*, 17(18):6933, 2020.
- [80] Zahra Nabizadeh-Shahre-Babak, Nader Karimi, Pejman Khadivi, Roshanak Rosshandel, Ali Emami, and Shadrokh Samavi. Detection of covid-19 in x-ray images by classification of bag of visual words using neural networks. *Biomedical Signal Processing and Control*, 68:102750, 2021.
- [81] Deng-Ping Fan, Tao Zhou, Ge-Peng Ji, Yi Zhou, Geng Chen, Huazhu Fu, Jianbing Shen, and Ling Shao. Inf-net: Automatic covid-19 lung infection segmentation from ct images. *IEEE Transactions on Medical Imaging*, 39(8):2626–2637, 2020.
- [82] Jun Ma, Yixin Wang, Xingle An, Cheng Ge, Ziqi Yu, Jianan Chen, Qiongjie Zhu, Guoqiang Dong, Jian He, Zhiqiang He, et al. Toward data-efficient learning: A benchmark for covid-19 ct lung and infection segmentation. *Medical physics*, 48(3):1197–1210, 2021.